Microfacies of the Upper Bird Spring Group (Pennsylvanian - Permian) arrow canyon range, Clark County, Nevaa

Autor(en): **Nowak, Frank J. / Carozzi, Albert V.**

Objekttyp: **Article**

Zeitschrift: **Archives des sciences [1948-1980]**

Band (Jahr): **25 (1972)**

Heft 3

PDF erstellt am: **12.07.2024**

Persistenter Link: https://doi.org/10.5169/seals-739380

MICROFACIES OF THE UPPER BIRD SPRING GROUP (PENNSYLVANIAN — PERMIAN) ARROW CANYON RANGE, CLARK COUNTY, NEVADA

BY

Frank J. NOWAK and Albert V. CAROZZI [1]

ABSTRACT

The upper 200 meters of the Bird Spring Group (Upper Missourian — Wolfcampian) were sampled at a vertical interval of 22 cm and 907 samples were collected. This part of the Bird Spring Group consists of a cyclic repetition of nine microfacies which are in order of general shallowing: a calcisiltite with scattered debris (microfacies 1), a mud-supported crinoidal calcarenite with either a micritic or a bioclastic matrix (microfacies 2), a grain-supported crinoidal calcarenite with a bioclastic matrix (microfacies 3), an oolitic calcarenite with cavity-filling sparry calcite cement (microfacies 4), a grain-supported brachiopod calcarenite with a calcisiltite matrix (microfacies 5), a mud-supported brachiopod calcarenite with a calcisiltite matrix (microfacies 6), a fine-grained pelletoidal calcarenite with a calcisiltite matrix (microfacies 7), a pelletoidal and foraminiferal calcarenite with a calcisiltite matrix which is usually recrystallized to pseudospar (microfacies 8), and a finely laminated calcisiltite (microfacies 9), often containing desiccation chips.

The following microscopic parameters were measured: frequency and clasticity of crinoid fragments, oolites, lithoclasts, and detrital quartz, and frequency of brachiopod debris, bryozoan debris, agglutinated foraminifers, calcispheres, and pellets (fecal and lithic). These data were computer plotted alongside a columnar section as variation curves showing stratigraphic behavior of the parameters. Combination of these measurements with the above microfacies classification led to a relative bathymetric curve wich represents a final interpretation of the oscillations of water depth during deposition.

The final environmental model consists of a seaward slope which grades into a discontinuous crinoidal bar and into a lagoon behind the bar. Microfacies 1 and 2 are found on the seaward slope where crinoids are the most abundant benthonic organisms although brachiopods and fusulinids are relatively abundant. The crinoidal bar is characterized by microfacies 3 and 4. This is the area of highest environmental energy and is the source of most bioclasts found in the other microfacies. Crinoids, bryozoans, red algae, and lithoclasts are the most important constituents and at times agglutinated and arenaceous foraminifers and pellets are relatively abundant. Microfacies 5 and 6 are found on the back slope of the crinoidal bar and contain the peak brachiopod frequency. The lagoon behind the bar, characterized by microfacies 7 and 8, contains pellets, agglutinated foraminifers, and lithoclasts of pelletoidal micrite formed by nearshore intraformational reworking. Microfacies 9 is found in the shoreward portion of the lagoon; it is usually laminated and contains flat micritic desiccation chips.

[1] Department of Geology, University of Illinois at Urbana — Champaign, Illinois, U.S.A. This paper is part of a doctoral thesis completed by F.J.N. under the supervision of A.V.C. and submitted to the Graduate College in September 1972.

The regressive sequence which started in the Atokan continues through the Wolfcampian, and the pattern of cyclic sedimentation found in the lower part of the Bird Spring Group also occurs in the investigated section. However the 12 cycles recognized in it display a similar amplitude indicating no trend toward further shallowing.

RÉSUMÉ

Les deux cents mètres de la partie supérieure du Bird Spring Group (Mississippian supérieur à Wolcampian) ont été soumis à une étude pétrographique détaillée comportant l'examen de 907 coupes minces séparées par un interval vertical moyen de 22 cm. Cette partie du Bird Spring Group est formée par la répétition cyclique de 9 microfaciès qui sont les suivants par ordre décroissant de profondeur générale de dépôt: calcisiltite à débris organiques disséminés (microfaciès 1), calcarénite crinoïdale à grains non jointifs et matrice micritique ou bioclastique (microfaciès 2), calcarénite crinoïdale à grains jointifs et matrice bioclastique (microfaciès 3), calcarénite oolithique à ciment sparitique de remplissage (microfaciès 4), calcarénite à brachiopodes à grains jointifs et matrice calcisiltique (microfaciès 5), calcarénite à brachiopodes à grains non jointifs et matrice calcisiltique (microfaciès 6), calcarénite pelletoïdale fine à matrice calcisiltique (microfaciès 7), calcarénite pelletoïdale à foraminifères et à matrice calcisiltique généralement recristallisée en pseudosparite (microfaciès 8), calcisiltite à texture finement rubanée contenant souvent des copeaux de dessication (microfaciès 9).

Les paramètres microscopiques suivants ont été mesurés: indices de fréquence et de clasticité des fragments de crinoïdes, oolithes, lithoclastes et quartz détritique; indice de fréquence des débris de brachiopodes et de bryozoaires, des foraminifères agglutinants, calcisphères et pellets (fécales et lithiques). Les variations stratigraphiques de toutes ces données ont été tracées sous forme de courbes par ordinateur. L'interprétation finale du milieu de dépôt exprimée par une courbe bathymétrique relative a été obtenue en combinant les variations des paramètres microscopiques avec la classification des microfaciès décrite plus haut.

Le modèle de l'environnement de sédimentation comporte une pente sous-marine qui s'élève vers une barre discontinue à crinoïdes à l'abri de laquelle s'étend une lagune. Les microfaciès 1 et 2 représentent la pente sous-marine où les crinoïdes sont les plus abondants composants benthoniques bien que les brachiopodes et les fusulinidés soient relativement fréquents. La barre à crinoïdes est caractérisée par les microfaciès 3 et 4. Elle correspond au milieu à énergie maximale et représente la source de la plupart des bioclastes dispersés dans les autres microfaciès. Les crinoïdes, bryozoaires, algues rouges et lithoclastes sont les composants les plus importants et parfois les foraminifères arénacés et agglutinants ainsi que les pellets sont relativement abondants. Les microfaciès 5 et 6 se trouvent sur la pente interne de la barre à crinoïdes et correspondent à la fréquence maximale des brachiopodes. La lagune, à l'abri de la barre, représentée par les microfaciès 7 et 8, contient des pellets, des foraminifères agglutinants et des lithoclastes de micrite pelletoïdale formés par des remaniements intraformationnels en bordure de côte. Le microfaciès 9 correspond à la partie côtière de la lagune, il est en général à texture rubanée et contient des copeaux micritiques de dessication.

La séquence régressive qui a débuté à l'Akotan se poursuit pendant le Wolfcampian et le type de sédimentation cyclique qui caractérise la partie inférieure du Bird Spring Group se rencontre également dans la série étudiée. Cependant les 12 cycles qui la constituent montrent une amplitude constante ce qui n'indique aucune tendance vers des conditions de moins en moins profondes du milieu de dépôt.

INTRODUCTION

This paper is part of a continuing detailed stratigraphic, paleontologic, and petrographic investigation of rocks in the Arrow Canyon Range being undertaken by A. V. CAROZZI, R. L. LANGENHEIM, Jr., and their students.

The Bird Spring Group (Mississippian-Permian) is a thick limestone sequence which displays a step-like pattern of alternating benches and slopes in the field characteristic of cyclic sedimentation. The present study deals with the upper 200 meters of the Bird Spring Group and is a continuation of previous investigations (HEATH, LUMSDEN and CAROZZI, 1967) which dealt with the lower 562 meters.

The studied section was sampled at an average vertical interval of 22 cm. In addition a 15 meter section was continuously sampled for the purpose of testing the suitability of 22 cm sampling interval for the present study. Thin sections made from these samples were investigated petrographically and subdivided into 9 carbonate microfacies using textural and microfaunal criteria. Average values of measured parameters were coded and plotted for each microfacies. The nine microfacies represent an ideal sequence which was used for an interpretation of the investigated section. The sequence, 1 through 9, represents a general shallowing, going up a seaward slope, across a discontinuous crinoidal bar and into a shallow lagoon. Variation curves of size and frequency of detrital and organic components were plotted alongside the stratigraphic column. An interpretative curve expressing the relative bathymetry was drawn: from this curve cyclic sedimentation comparable to that found in lower portions of the Bird Spring Group is interpreted.

LOCATION

Samples used in this investigation were collected in Arrow Canyon, located in the Arrow Canyon quadrangle which is bounded by latitude 36° 30′ N and latitude 36° 45′ N and longitude 114° 45′ W and longitude 115° W, approximately 50 miles northeast of Las Vegas, Nevada. Maximum elevation above sea level is 5032 feet; and minimum elevation in the valley is less than 2000 feet, giving a total relief of over 3000 feet. Broad valleys with playa lake beds and large alluvial fans separate the Arrow Canyon Range from the Las Vegas Range on the west and the more distant Mormon Range on the east.

Arrow Canyon trends east-west and is superposed across the northern end of the Arrow Canyon Range (Figure 1). The Pennsylvanian-Permian rocks studied are in the upper part of the Bird Spring Group and are exposed in the lower, more open part of Arrow Canyon. The Bird Spring Group rests disconformably on Mississippian Monte Cristo Limestone and is truncated at the top by the present topographic surface. The rocks sampled dip approximately 40° to the east and are on the northeastern limb of a partially overturned syncline. The syncline itself is bounded to the northwest by a major thrust fault. The rugged topography, extreme aridity,

and lack of soil and vegetation lead to the presence of a nearly continuous exposure for sampling.

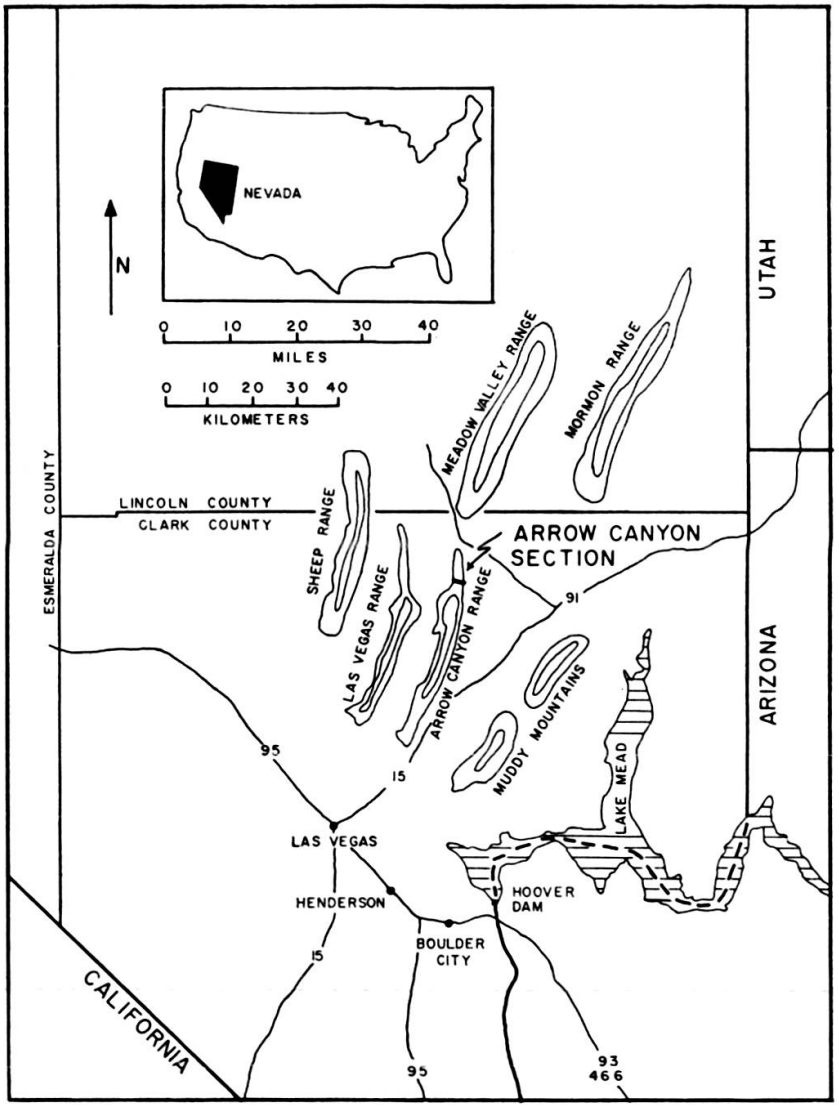

FIG. 1. — Location Map

TECTONIC SETTING

The Paleozoic section at Arrow Canyon was deposited in the Bird Spring Basin which is part of the Millard miogeosynclinal belt of KAY's cordilleran orthogeosyncline (KAY, 1947). During Late Paleozoic, the miogeosyncline was not a simple, linear, subsiding trough, but rather a complex mosaic of positive and negative features, some inter-connected, others not (DOTT, 1958; BISSELL, 1962; BRILL, 1963; RICH, 1969, 1971). The line of demarcation between miogeosyncline and eugeo-

syncline on the west generally is called the Antler orogenic belt or the Manhattan Line (BISSELL, 1962; BRILL, 1963; RICH, 1969, 1971). An eastern boundary, separating miogeosynclinal from platform facies is the Las Vegas-Wasatch Line (WELSH, 1959; BISSELL, 1962). Platform facies are more arenaceous and contain more prominent unconformities than do miogeosynclinal facies (WELSH, 1959).

STRATIGRAPHY

Because of a complex tectonic setting, a controversy in the naming, subdivision, and correlation of many Late Paleozoic units exists in the Great Basin (WELSH, 1959; BISSELL, 1962; BRILL, 1963). In Arrow Canyon Range, the Bird Spring Group is

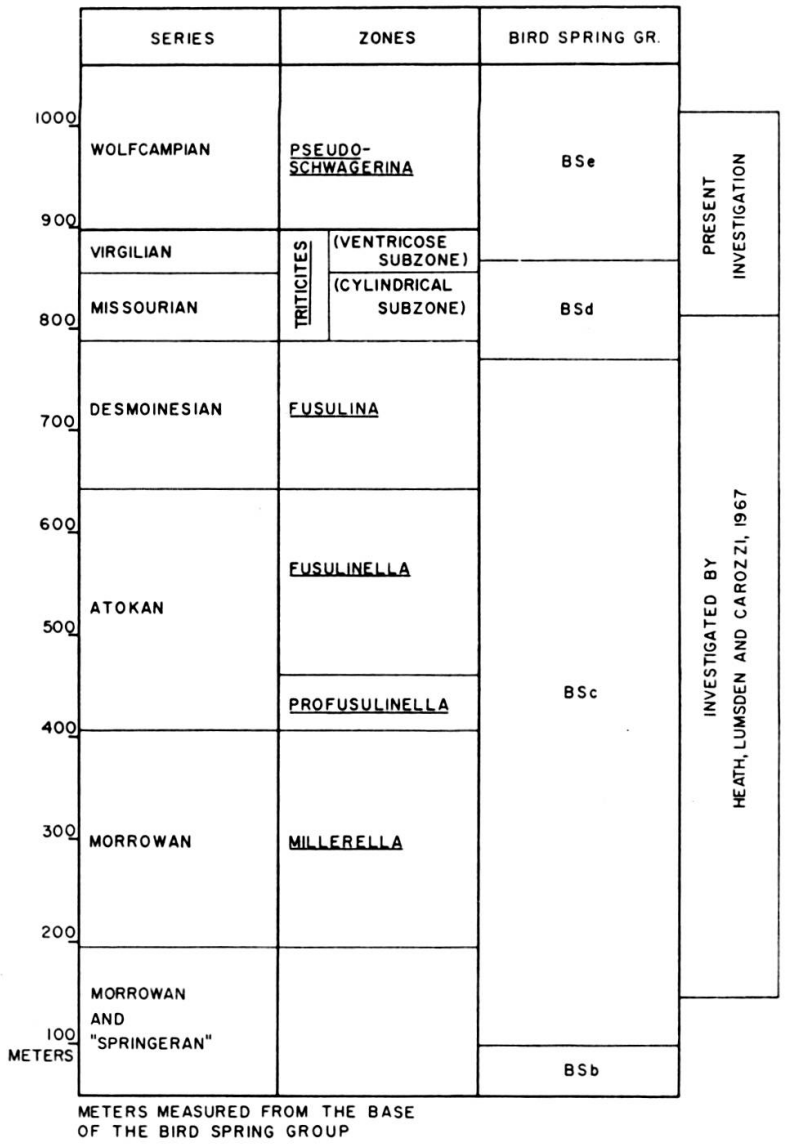

FIG. 2. — Biostratigraphy of the Bird Spring Group at Arrow Canyon and Extent of Microfacies Studies

the uppermost Paleozoic unit. For a review of the problem of correlation and subdivision of this unit the reader is referred to earlier stratigraphic work in this area (LANGENHEIM *et al.*, 1962; LANGENHEIM and LANGENHEIM, 1965; WEBSTER, 1969).

To be consistent with previous petrographic work done at Arrow Canyon, this study will use terminology proposed by LANGENHEIM *et al.* (1962) and LANGENHEIM and LANGENHEIM (1965).

The Bird Spring Group at Arrow Canyon is approximately 1066 meters thick and is subdivided into five locally useful, informal units; BSa, BSb, BSc, BSd, BSe.

The lowest unit, BSa, has been elevated to formational rank as the Battleship Wash Formation (LANGENHEIM and LANGENHEIM, 1965). It is 24 meters thick and consists of cherty, arenaceous limestone and calcareous sandstone. It rests disconformably on the Chesterian Monte Cristo Limestone.

Unit BSb is 74 meters thick and consists of red and black shale, argillaceous and arenaceous limestone, and micaceous sandstone.

Unit BSc is approximately 675 meters thick and is mainly limestone although chert and calcareous shale and sandstone occur in cyclic alternation.

Unit BSd, 98 meters thick, is composed of thickly bedded resistant limestone which alternates with easily eroded, nodular, shaly, cherty limestone.

Unit BSe is 162 meters thick, of which the lower 3/5 is thickly bedded dolomite and the upper 2/5 is limestone and interbedded dolomite.

This study begins 816 meters above the base of the Bird Spring Group and 43 meters above the base of the BSd. The uppermost unit is 1016 meters above the base of the Bird Spring Group and 145 meters above the base of the BSe.

Work of P. E. CASSITY (1965) and of CASSITY and LANGENHEIM (1966) has geologically dated the section. The base of the studied section is 54 meters above the Desmoinesian-Missourian boundary. The Missourian-Virgilian and Virgilian-Wolfcampian boundaries are within the studied section (Figure 2).

PREVIOUS PETROGRAPHIC INVESTIGATIONS

The lower and middle portions of the Bird Spring Group at Arrow Canyon have been studied (HEATH, LUMSDEN and CAROZZI, 1967) in a manner similar to the present study. Because their work is closely related to the present study, a comparison of the respective terminologies is necessary.

HEATH *et al.*, recognized a microfacies 0 which is a calcisiltite essentially devoid of organic debris. Several samples in the present study could fit into this category but were not numerous enough to warrant a separate microfacies. Therefore they were placed in microfacies 1.

Microfacies 1, 2, and 3 in the two works are similar. However, in the present study microfacies 2 and 3 are specifically defined as crinoidal calcarenites, mud- and

grain-supported, whereas in previous work no faunal criteria were used for placing samples in these categories.

Microfacies 4 in the present study is an oolitic calcarenite with sparry calcite cement and is equivalent to microfacies 5 of HEATH *et al.* Previous workers also have a biocalcarenite with a sparry calcite cement, their microfacies 4, which is not found in the present study.

In addition, HEATH *et al.*, recognize quartz-rich samples and assign them to microfacies 0a, 1a, 2a, 3a and 4a. These are equivalent to their microfacies 0-4 except that these groups contain more than 10% detrital quartz. Several samples in the present study display a similar amount of detrital quartz but are not numerous enough to justify the establishment of separate microfacies.

No equivalents of microfacies 5-9 of the present study exist in the work of HEATH *et al.*

METHODS AND TECHNIQUES

Petrographic Analysis

In the field 907 hand specimens were collected from a stratigraphic interval 200 meters thick, and 175 field units were distinguished. Vertical spacing of samples normally was primarily a function of lithology, and averaged approximately 22 cm. In addition, a 15 meter section (176 samples) was collected to approximate a continuous section. The purpose was to attempt to determine statistically an optimum sampling interval so that no environmentally significant microfacies would be missed.

Thin sections were cut to a thickness slightly above a standard value of 0.03 mm to allow better contrast among microscopic components.

Thin sections were studied following the method proposed by CAROZZI (1950, 1958, 1961) which consists of tabulating the indices of clasticity and frequency of all detrital components, and a frequency index of all the benthonic and pelagic organic components (intact or as bioclasts) of a carbonate rock. This is followed by an interpretation based on a relative bathymetric curve or a relative energy level curve expressing environmental variations of carbonate deposition through time.

The index of clasticity for any given component in a thin section is defined as the maximum diameter of that component. As we are dealing with an apparent diameter, except in the particular case where a section is cut through the center of a grain, the index of clasticity is consistently less than the maximum diameter. In order to obtain some degree of constancy in the measurement of the index of clasticity, the six largest grains in a particular thin section were selected and their diameters averaged. Occasional isolated grains notably larger than grains commonly making up the rock were considered to result from minor variations in agents of deposition not rep-

resentative of the overall environment. And hence, though isolated larger diameters were measured, they were not entered into tabulation of the index of clasticity.

The final expression of the index of clasticity is a numerical figure, given in millimeters, which represents the largest diameter of a grain that could be set in motion by the average forces acting in the environment of deposition.

The frequency index of a given component is defined as the number of its particles present in any given area of a thin section. In practice, this requires counting the number of grains found over a constant area on each thin section. The number must be on the order of at least 100 particles so that measurement will be statistically reliable. A problem arises with the determination of the frequency. If a rock is made up predominantly of closely packed grains of a particular clastic component, then,

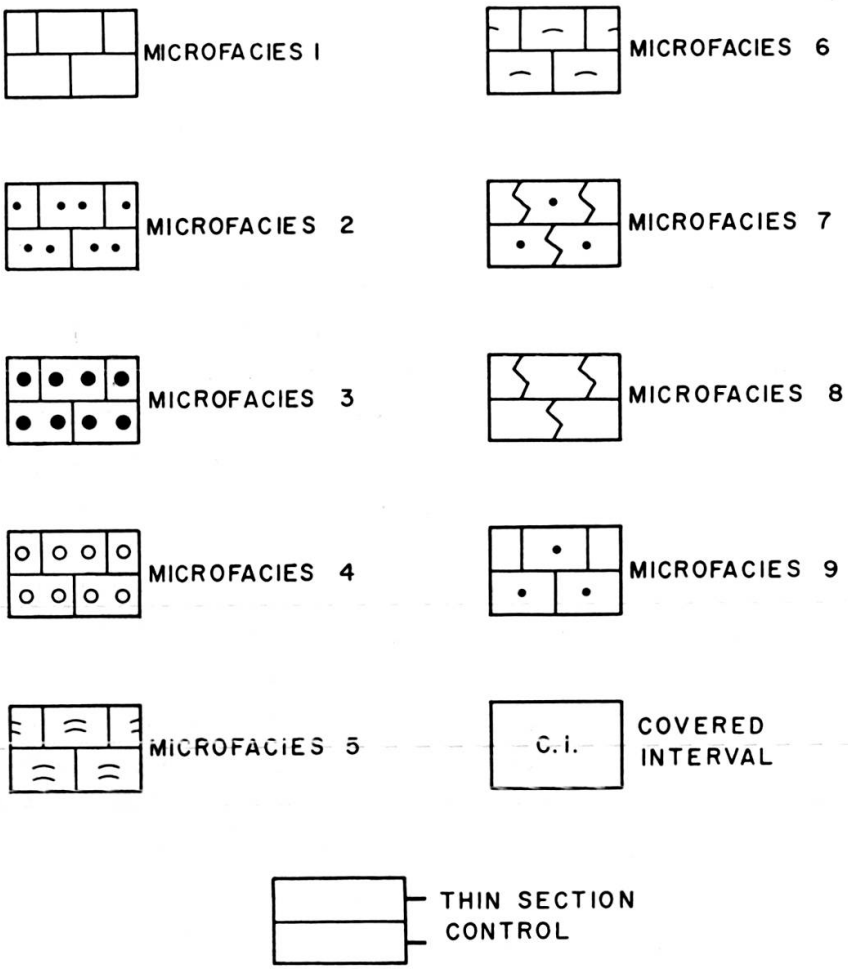

FIG. 3. — Table of Symbols

as the grain size increases the frequency index will decrease, thereby giving a misleading value. In order to overcome this disadvantage, an area was selected for each clastic component which had a diameter of at least 10 times the average diameter of that component. In the present study, standard surface areas used for frequency of

crinoids, brachiopods, bryozoans, calcispheres, lithoclasts, and oolites was 181.2 mm^2 whereas for pellets, agglutinated foraminifers, and detrital quartz, standard area was 30.9 mm^2.

The curves expressing stratigraphic variations of measured parameters were drawn by Calcomp plotter (Figures 12-20).

Thin sections were assigned to microfacies on a basis of microscopic textures and relative abundance of organic and inorganic constituents. To the right of each set of variation curves, microfacies have been arranged from left to right in order of decreasing relative water depth. Even though spacing is constant, this does not imply a constant rate of relative depth decrease. Actually, depth differences between some adjacent microfacies may be small.

The scale, 1 through 9, can also be interpreted as representing relative distance from shore, with microfacies 1 being farthest. No attempt has been made to display environmental energy because no simple relationship was established between relative environmental energy and depth of water in the interpretative model.

Statistical Analysis and Computer Techniques

Analysis of petrographic data for this study was expedited by application of computer techniques. Digital computer facilities at the University of Illinois, Urbana, consisting of an IBM 360/75 computer were used for all computations. Petrographic data were plotted against their vertical stratigraphic position on 73 centimeter-wide paper by a Calcomp 763 Zip Mode Plotter using a modification of a previously written program (Rao, 1970, Rao and Carozzi, 1971). Coded average values were plotted on 28 centimeter-wide paper using a FORTUOI plotting subroutine (CSO Fortran Library, University of Illinois).

Before the average values were plotted they were standardized using the following formula.

$$Z = \frac{(\overline{Y} - \mu)}{\sigma}$$

Z is a standardized average; $\overline{Y}$ is the average value for one parameter in one microfacies; μ is the average for that component using all samples; σ is the standard deviation of that component for all samples.

An advantage of coding data in this manner is that Z values for any component will have a mean of 0 and a standard deviation of 1. This facilitates graphic presentation of the data and allows easy comparison of variation of the average values even though uncoded averages may vary greatly.

After all thin sections were grouped into microfacies and their parameters measured, the 15 meter continuous sampling section was analyzed. Data were picked

from the continuous section at approximately 20 cm intervals and these samples were used in plotting of variation curves for the entire section. Average thickness of microfacies identified at a 20 cm sampling interval is 46 cm. When all samples from the continuous section were considered, average thickness of microfacies identified is 20 cm. Statistical analysis indicates that a significant difference exists between the average microfacies thickness using a 20 cm interval and average thickness using a continuous sampling (Appendix).

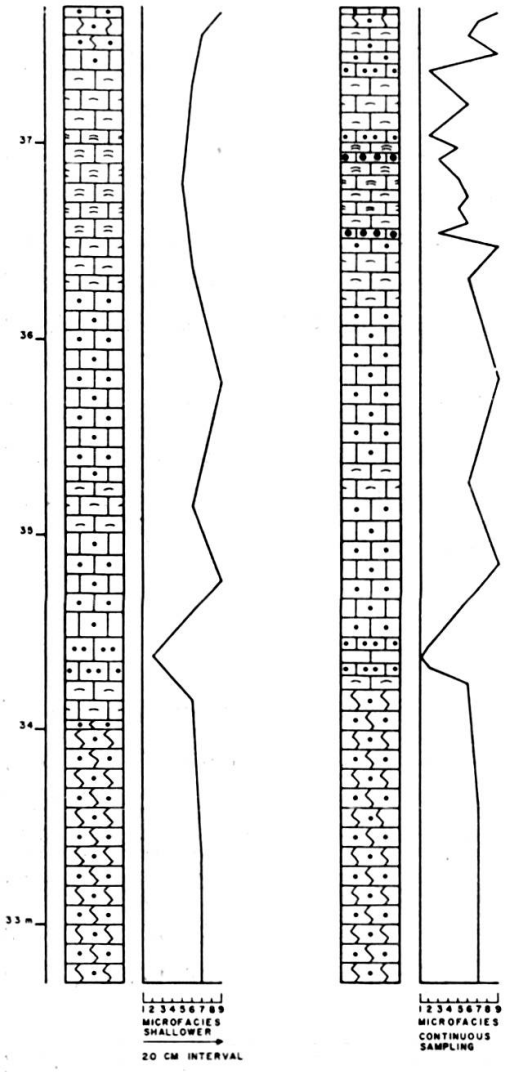

FIG. 4. — Comparison of Results Between Different Sampling Techniques

To illustrate the difference between the results obtained using these two sampling procedures, a 5 meter portion of the continuous section was chosen at random and microfacies identified by the two sampling procedures were plotted at their proper stratigraphic position (Figure 4).

A definite statement about the practical significance of the difference between the two curves is difficult to make. Continuous sampling picks up greater variation, but the overall trend of both curves is similar. The amount of environmental information gathered from the two methods is different, however 20 cm sampling interval seems adequate for the type of carbonate sedimentation investigated.

COMPONENTS

A limit between carbonate skeletal material and matrix material was set arbitrarily at 60 microns because of a difficulty of identifying and counting skeletal debris below that size.

Major Organic Components

Crinoids are the most abundant biogenic component, occurring both as columnals and plate fragments. Other echinoderm debris, with the exception of echinoid

spines, were counted as crinoid fragments. Because crinoid fragments behave as detrital particles their clasticity index was measured also.

Brachiopods and bryozoans occur in most slides. Larger brachiopod fragments were identified easily by their arcuate shape and characteristic shell structure. Likewise, larger bryozoan debris were recognized by the shape of zooecia and fibrous wall structure. Positive identification was not possible for small fibrous fragments; therefore they arbitrarily were included in the brachiopod frequency count. Consequently, the brachiopod frequency is biased slightly.

Agglutinated foraminifers occur in all microfacies but are concentrated in microfacies 7 and 8. They were distinguished from pellets by their more irregular shape and the presence of an internal structure. As shown by MAMET (1970) the frequent underestimation in the literature of the abundance and importance of agglutinated foraminifers in carbonate environments should also be stressed here.

Calcispheres, behaving as pseudo-pelagic organisms, are found in all microfacies. They were identified easily by their dark rim and sparry calcite interior.

Minor Organic Components

Minor components are: ostracods, pelecypods, gastropods, trilobites, fusulinids, arenaceous foraminifers, *Dasycladaceae*, and *Archaeolithophyllum* (WRAY, 1965). Their presence or absence was used for the interpretation of the microfacies but a frequency index was not calculated. These components showed no particular distribution pattern with the exception of fusulinids and arenaceous foraminifers. The former are present in most microfacies but showed strong affinities for microfacies 2, 5, and 6. Likewise, the arenaceous foraminifers, although common, are most frequent in microfacies 3.

Inorganic Components

Pellets, both fecal and lithoclastic in origin are the most abundant inorganic component. A value of 0.15 mm (FOLK, 1962) was used to separate pellets from lithoclasts. In some cases, the pellet frequency curve is not representative of the true number of pellets in a slide because merging of pellets makes accurate counting virtually impossible.

Lithoclasts, rounded to subangular, and reaching several millimeters in diameter, occur in all microfacies except microfacies 1. They either originated from intraformational reworking or represent flat desiccation chips transported from shallower areas.

Oolites were found in only one field unit. Oolitization was not very intense, most of the oolites being superficial (CAROZZI, 1960). Oolite cores are either bioclasts or small lithic fragments.

Quartz occurs both as detrital grains and secondary crystals. The latter were not counted unless a core of detrital quartz was identifiable.

MICROFACIES DESCRIPTION

The recognized microfacies are described in order of general shallowing; their precise environmental relationships will be discussed later.

Microfacies 1

Calcisiltite with scattered sand-size bioclasts (Plate 1, A). Samples from this group grade from pure silt-size calcareous mud to ones in which identifiable bioclasts reach approximately 20%, this value being the lower limit for microfacies 2.

The groundmass consists primarily of silt-size grains of carbonate material in which are often scattered small dolomite rhombs (determined by staining) and minute angular grains of detrital quartz.

The predominant organic components are small angular fragments of crinoids, brachiopods, and bryozoans associated with rare fusulinids.

Microfacies 2

Mud-supported biocalcarenite with either micritic or bioclastic matrix, both of which may be pelletoidal (Plate 1, B).

Crinoid fragments dominate over brachiopods, bryozoans, ostracods, and fusulinids. The bioclasts are randomly scattered throughout the matrix but in places their reworking by scavengers leads to areas with a grain-supported texture. Silt-size detrital quartz is usually present but is not as abundant as in microfacies 1.

Microfacies 3

Grain-supported biocalcarenite with bioclastic matrix, at times pelletoidal, with both fecal and lithic pellets (Plate 1, C). In several slides no clear distinction was possible between bioclasts and matrix because of a continuous gradation from larger bioclasts to fine silt-size debris, too small to identify. Pressure-solution contacts between components and reworking by scavengers further complicate the petrographic identification.

Crinoids reach their peak frequency in this microfacies and dominate over all other biogenic components. Towards the top of the investigated section arenaceous foraminifers, such as *Endothyra*, and agglutinated foraminifers become more important constituents. Angular grains of detrital quartz are uniformly present.

Microfacies 4

Oolitic calcarenite with cavity-filling sparry calcite cement (Plate 1, D). Superficial oolites largely predominate over normal oolites with several concentric layers. The cores of the oolites are either bioclasts, usually crinoids or brachiopods, or rounded micritic grains with or without organic debris.

Rounded lithoclasts of fossiliferous micrite are the most common detrital components next to the oolites. Non-oolitized fragments are present but in fewer number than in other microfacies. Detrital quartz is absent.

Microfacies 5

Grain-supported brachiopod calcarenite with calcisiltite matrix (Plate 1, E). Shell fragments and spines, associated with crinoids and bryozoans, are usually arranged parallel to bedding, indicating a bioaccumulated character. In some instances though, scavenger action has introduced appreciable disruption of the original texture. Angular grains of detrital quartz are also usually present.

Microfacies 6

Mud-supported brachiopod calcarenite which differs from microfacies 5 mainly by the smaller amount of sand-size organic debris (Plate 1, F). The brachiopod shells are also normally aligned with the bedding although disturbances through reworking by scavengers are frequent.

Microfacies 7

Fine-grained pelletoidal calcarenite with calcisiltite matrix (Plate 2, A, B). The pellets are mainly fecal in origin; often their merging makes the distinction of individuals virtually impossible.

Scattered among the pellets are sand-size debris of crinoids, brachiopods and bryozoans; occasionally agglutinated foraminifers are relatively abundant. Angular grains of detrital quartz are usually present.

Microfacies 8

Fine-grained pelletoidal and foraminiferal calcarenite with micrite matrix, usually recrystallized to pseudospar (Plate 2, C, D).

Agglutinated foraminifers and fecal pellets are the most important constituents although most of the other organic components occur in minor quantities. Lithoclasts, mainly of finely pelletoidal micrite originating from microfacies *7*, are abundant. Detrital quartz is present in most slides.

Microfacies 9

Calcisiltite with irregularly scattered debris of fine sand-size crinoids and brachiopods (Plate 2, E, F).

This microfacies is commonly finely laminated with quartz-rich layers and flat desiccation chips of micrite which formed in an assumed adjacent tidal flat. Compositionally microfacies 9 and 1 are very similar but textural differences are important enough to make them easily distinguishable.

PARAMETER VARIATIONS

The average measured frequencies and clasticities of the components of the nine microfacies (Table 1) have been plotted after having been coded following the previously described method.

Microfacies 1 (Figure 5) is below average in all measured parameters except for the frequency of detrital quartz.

Microfacies 2 and 3 (Figure 5) show an increase in the values of most measured parameters and the importance of crinoids in particular. There is a small brachiopod frequency peak in microfacies 2, and in microfacies 3 the bryozoan peak is evident.

In microfacies 4 (Figure 6), oolitization leads to a reduction of the values of all parameters except lithoclast frequency and bryozoan frequency. The high bryozoan frequency is not ecologically controlled because these organisms occur as detrital particles.

Microfacies 5 and 6 (Figure 6) are dominated by an abundance of brachiopods.

Microfacies 7 and 8 (Figure 7) show strong concentrations of agglutinated foraminifers and pellets, furthermore, microfacies 8 has a peak of lithoclast frequency.

Microfacies 9 (Figure 7) is almost identical to microfacies 1, confirming the visual compositional similarity observed under the microscope.

TABLE I

Average Values of Parameters by Microfacies

	Microfacies								
Components	1	2	3	4	5	6	7	8	9
Crinoid Frequency	65	207	222	87	117	132	156	127	65
Crinoid Clasticity (mm)	0.46	0.58	0.79	0.96	0.71	0.43	0.49	0.53	0.37
Bryozoan Frequency	4	10	15	25	6	12	5	6	3
Brachiopod Frequency	38	126	80	40	295	242	53	43	60
Agglutinated Foraminifer Frequency	4	17	30	0	24	10	64	75	6
Pellet Frequency	2	17	30	22	18	18	534	306	18
Calcisphere Frequency	1	8	11	1	18	7	11	8	2
Lithoclast Frequency	0	5	20	104	2	2	12	97	1
Lithoclast Clasticity (mm)	0	0.04	0.17	0.89	0.10	0.01	0.13	0.45	0.13
Oolite Frequency	0	0	0	241	0	0	0	0	0
Oolite Clasticity (mm)	0	0	0	0.58	0	0	0	0	0
Quartz Frequency	164	92	101	2	104	140	86	53	176
Quartz Clasticity (mm)	0.04	0.05	0.05	0.01	0.05	0.07	0.05	0.05	0.05

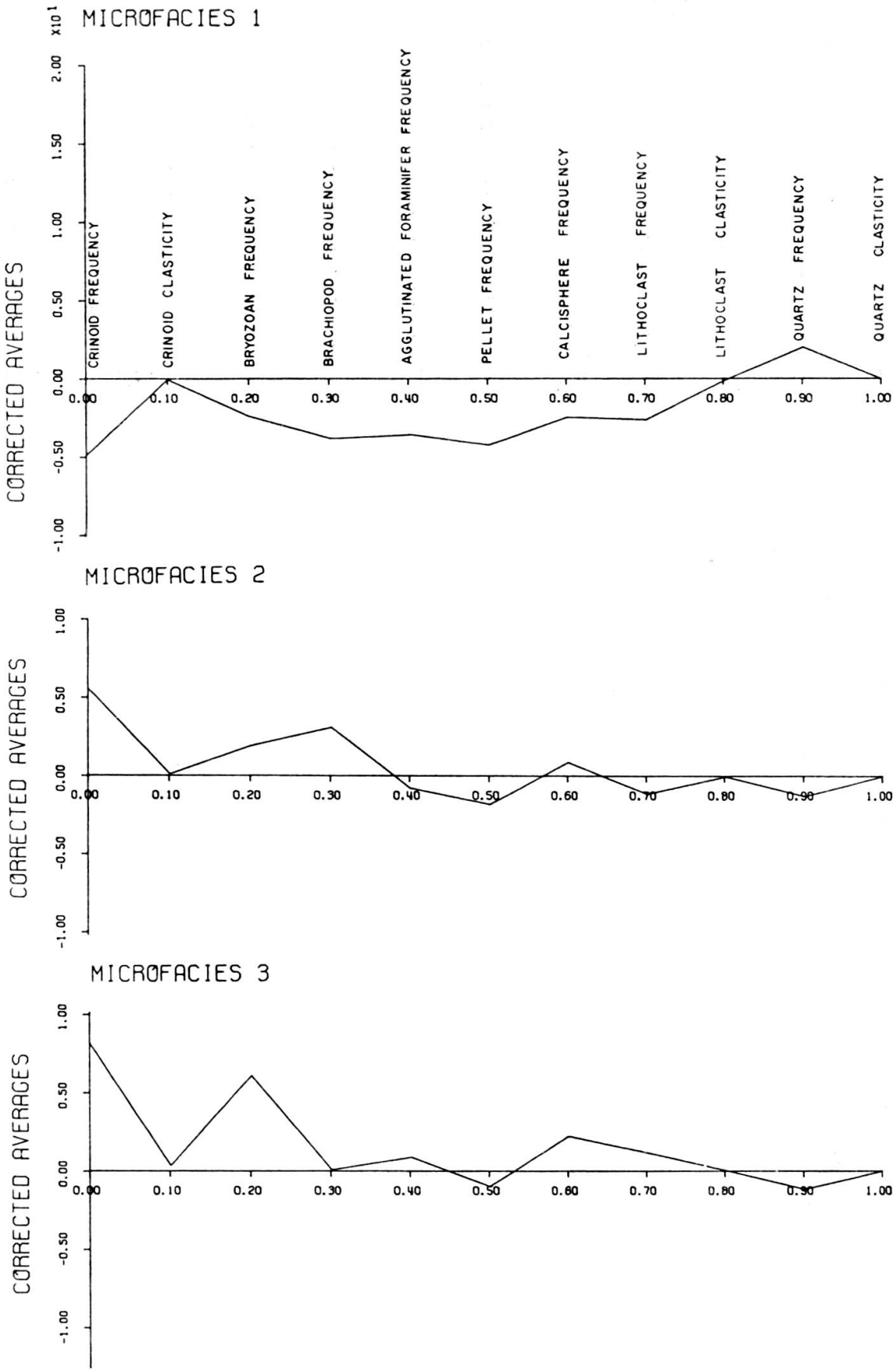

FIG. 5. — Coded Average Values of Parameters for Microfacies 1, 2, 3

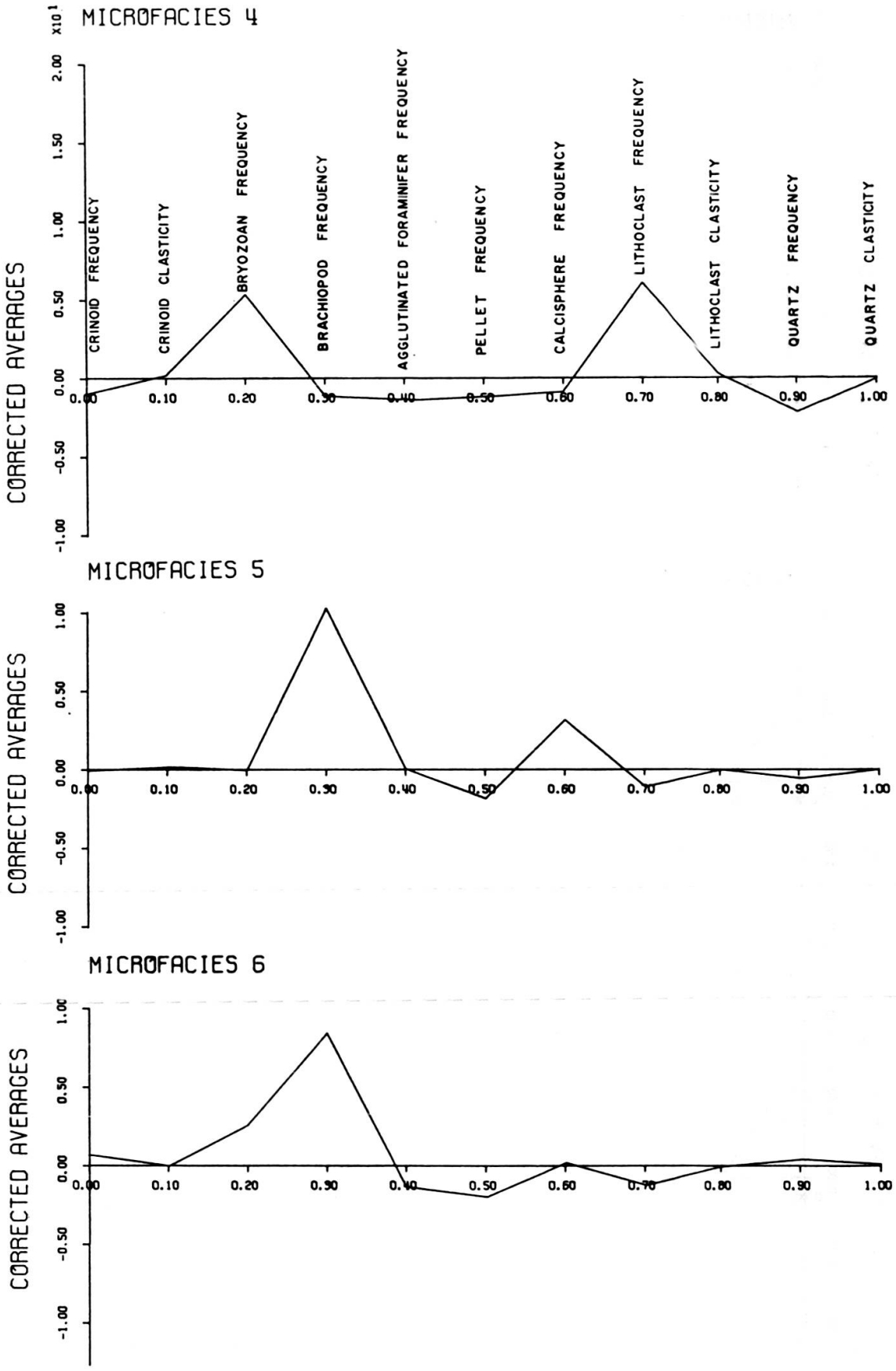

FIG. 6. — Coded Average Values of Parameters for Microfacies 4, 5, 6

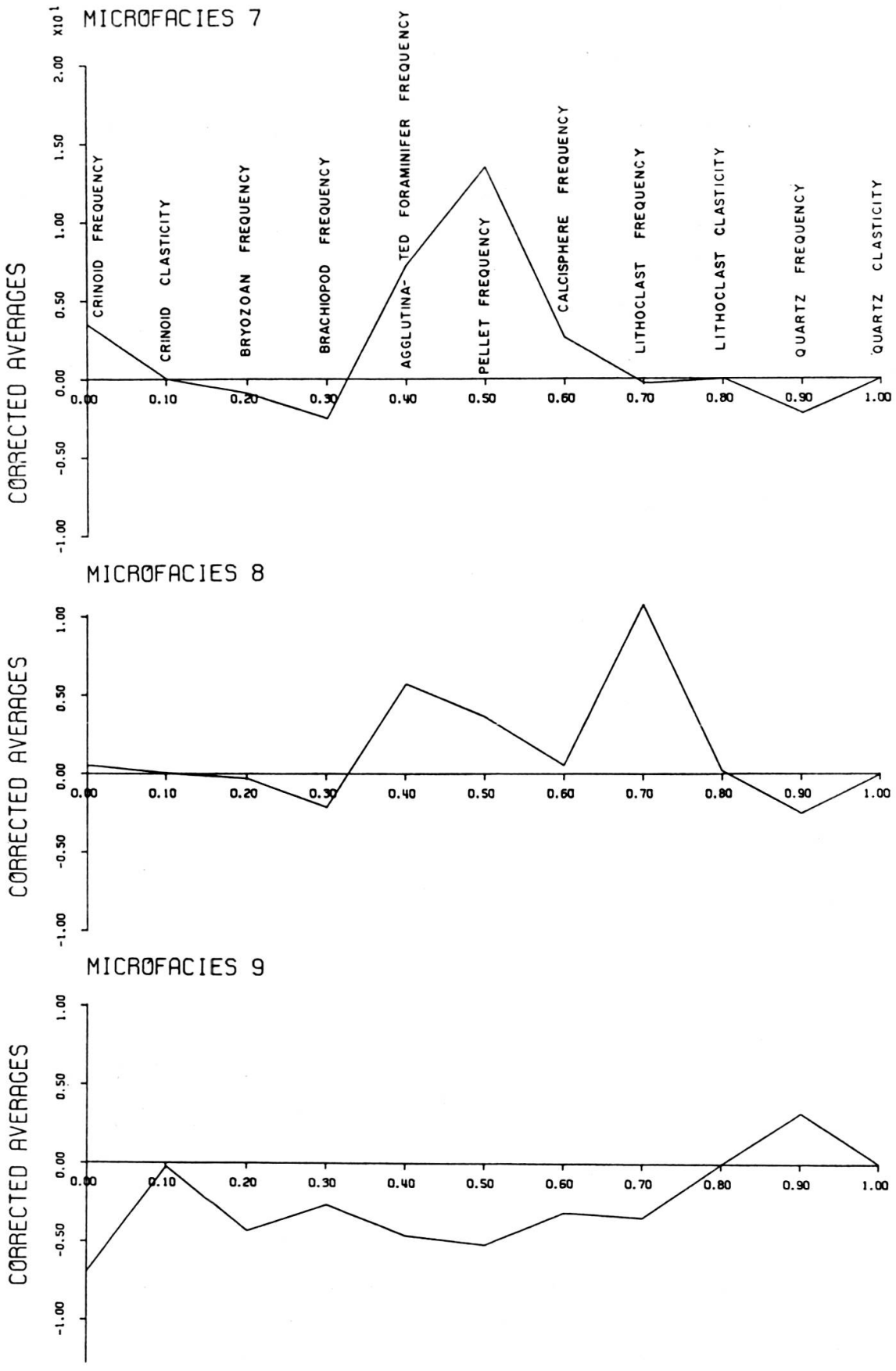

FIG. 7. — Coded Average Values of Parameters for Microfacies 7, 8, 9

IDEAL VERTICAL SEQUENCE

The nine microfacies described are interpreted to represent different environments of deposition which grade into one another vertically (Figure 8) and horizontally (Figure 11). Considered together they represent an inferred ideal sequence which may be used for the general interpretation of the investigated section. The sequence, 1 through 9, represents a general shallowing, going up a seaward slope, across a crinoidal bar made discontinuous by tidal channels, and into a shallow lagoon. No shoreward boundary of the lagoon was seen in the section studied. The lagoon probably graded into a carbonate tidal flat, as several slides from microfacies 9 contain desiccation chips apparently carried from such an adjacent environment.

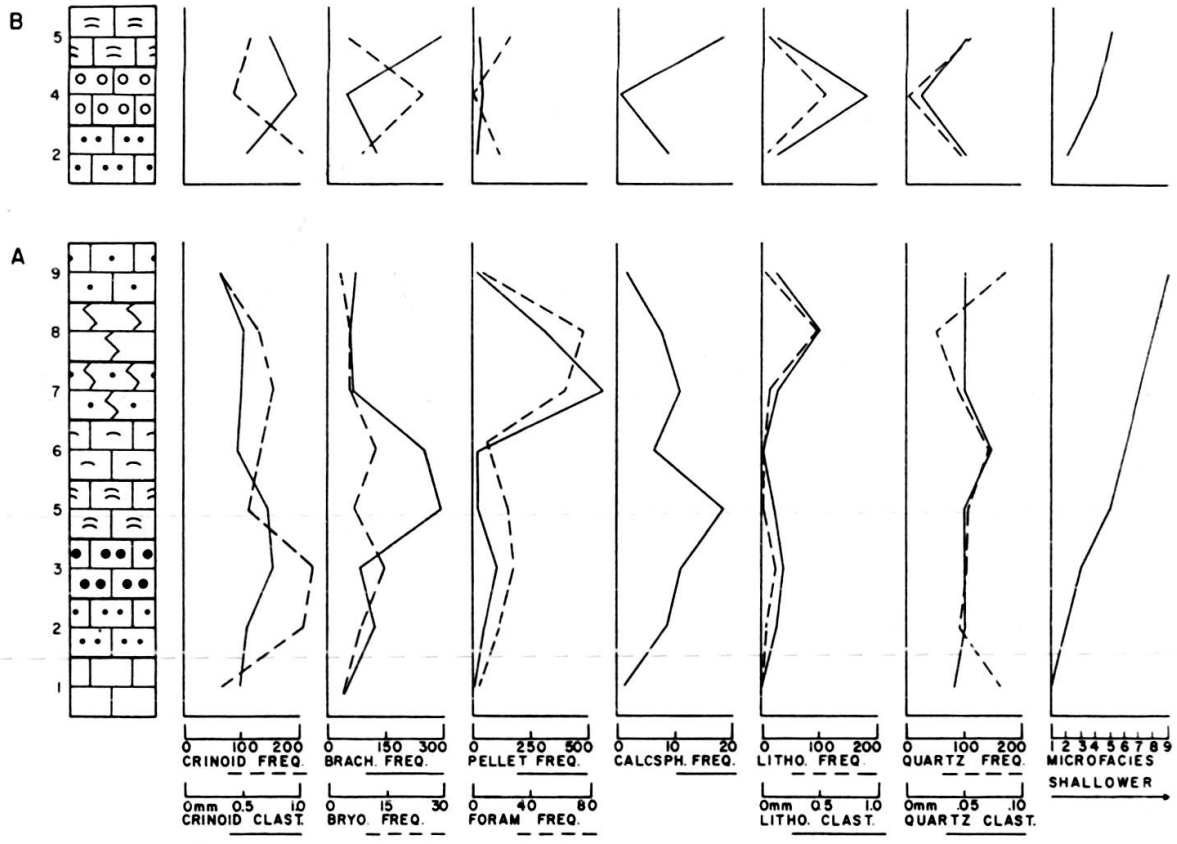

FIG. 8. — Parameter Variations for Ideal Vertical Sequence

The lithologic section (Figure 8, A) shows the superposition of microfacies 1 through 9. The thickness of each microfacies is arbitrary, no attempt has been made to show relative thicknesses. Because microfacies 4 is in the same position as microfacies 3 and represents a temporary period of oolite development, a portion of the ideal sequence, with microfacies 4 substituting for microfacies 3, is shown (Figure 8, B).

The curves express the variation of average frequency and clasticity through the different microfacies. The shapes of all curves are strongly influenced by the presence of the crinoidal bar.

Crinoid frequency increases from an average of 65 fragments in microfacies 1 to a peak of 222 in microfacies 3. It decreases to an average value of 117 in microfacies 5 and subsequently rises to a peak of 156 in microfacies 7. Crinoid clasticity and frequency curve shapes are similar. A maximum clasticity of 0.79 mm in microfacies 3 corresponds to the greatest frequency. After a decrease to 0.43 mm in microfacies 6, crinoid clasticity is essentially constant. The source of the crinoid fragments is inferred to be the bar itself. This accounts for the peak frequency in microfacies 3. Crinoids are then transported in either direction away from the bar by tidal currents washing across it. The small peak of crinoid frequency in microfacies 7 is caused by a concentration of transported particles in the lagoon.

The curve of brachiopod frequency shows a bimodal distribution, with a minor peak of 126 in microfacies 2 and a major peak of 295 fragments in microfacies 5. This is due to the brachiopods preferring the flanks of the crinoidal bar, especially the internal margin facing the lagoon (microfacies 5). In this area, a bioaccumulated texture may develop.

The bryozoan frequency curve shows no regular variation. However the presence of small peak values in microfacies 3 and 6 indicate a preference of bryozoans either for the crinoidal bar or the area immediately behind it.

The curve of pellet frequency shows a bimodal pattern with a minor peak in microfacies 3 and maximum concentration in microfacies 7. Two environments of pellet formation exist. In agitated conditions on the bar, lithic pellets are found in addition to fecal pellets. In the more quiet water conditions behind the bar, fecal pellets predominate.

The frequency curve of agglutinated foraminifers is similar to that of pellet frequency. A minor peak in microfacies 3 and a major peak in microfacies 8 would indicate two separate communities of agglutinated foraminifers with the larger of the two located behind the crinoidal bar. The location of the major community is consistent with the work of MAMET (1970) which places a majority of agglutinated foraminifers behind an oolitic bank.

Calcisphere frequency varies from 1 in microfacies 1, to 18 in microfacies 5. A small peak of 11 occurs in microfacies 7. The position of the calcisphere peaks does not make it clear whether they floated as pelagics over the bar from open sea conditions and settled behind it or originated in the lagoon behind the bar as algal spores.

Lithoclast frequency varies from 0 in microfacies 1 to 20 in microfacies 3. It decreases to an average value of 2 in microfacies 6 and jumps to 97 in microfacies 8. The clasticity curve almost parallels the frequency curve. Maximum frequency and clasticity of lithoclasts occur on the bar and in the lagoon behind it. The peak of

both curves in microfacies 3 represents the products of reworking processes on the crinoidal bar, the highest peak in microfacies 8 represents a near-shore intraformational reworking of microfacies 7.

The highest average values of detrital quartz frequency occur in microfacies 1 and 9. The peak in microfacies 9 expresses the proximity of an extrabasinal source of silt-size quartz. The concentration in microfacies 1 is due to the accumulation of fine silt-size quartz in deeper water in front of the bar after transit across the depositional environment. The minor peaks in quartz frequency and clasticity in microfacies 6 represent a pocket of slightly larger quartz grains which could not be transported over the crinoidal bar.

With development of an oolitic environment, microfacies 4 replaces microfacies 3 (Figure 8, B). The general effect is a reduction in average values of all measured parameters except crinoid clasticity, bryozoan frequency, pellet frequency and lithoclast frequency and clasticity due to the energy increase in an oolitic environment.

Presence of a crinoidal bar and a lagoon behind it have affected variations of average values of all measured parameters. All parameters, except those of brachiopods, calcispheres, and detrital quartz, have maximum values in one of these two environmental locations.

The curve to the extreme right (Figure 8) expresses the relative bathymetry of the environment of deposition. It shows a general shallowing going from microfacies 1 to microfacies 9.

HORIZONTAL ENVIRONMENTAL MODEL

The variation of coded average frequency for each component through the nine microfacies were plotted (Figures 9, 10).

Crinoid frequency (Figure 9) shows peaks in microfacies 3 and 7.

Bryozoan frequency (Figure 9) reaches maximum values in microfacies 3 and 5, however this curve has no definite trend.

The brachiopod frequency curve (Figure 9) is definitely bimodal with peaks in microfacies 2 and 5.

The curve of agglutinated foraminifer frequency (Figure 9) shows the presence of the two communities of these organisms in microfacies 3 and microfacies 7 and 8, with the latter being the larger of the two.

The coded average pellet frequency (Figure 10) for all microfacies except microfacies 7 and 8 is below 0 due to the large number of pellets in those microfacies. However there is still a small peak of pellets evident in microfacies 3.

The average calcisphere frequency (Figure 10) shows no definite trend.

The curve of lithoclast frequency (Figure 10) is bimodal with the two peaks in microfacies 3 and 8.

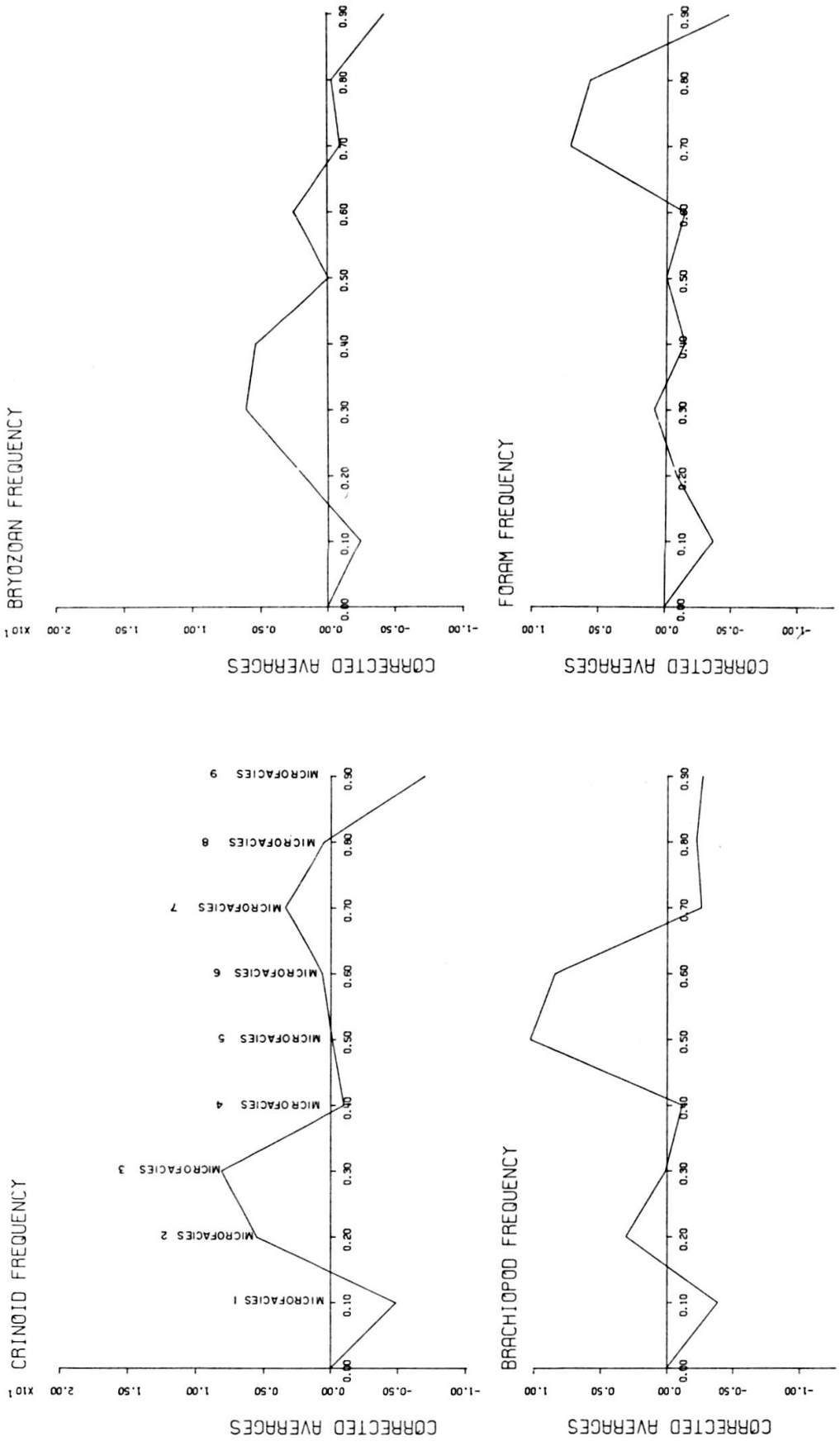

FIG. 9. — Variation of Coded Average Values of Parameters Through all Microfacies

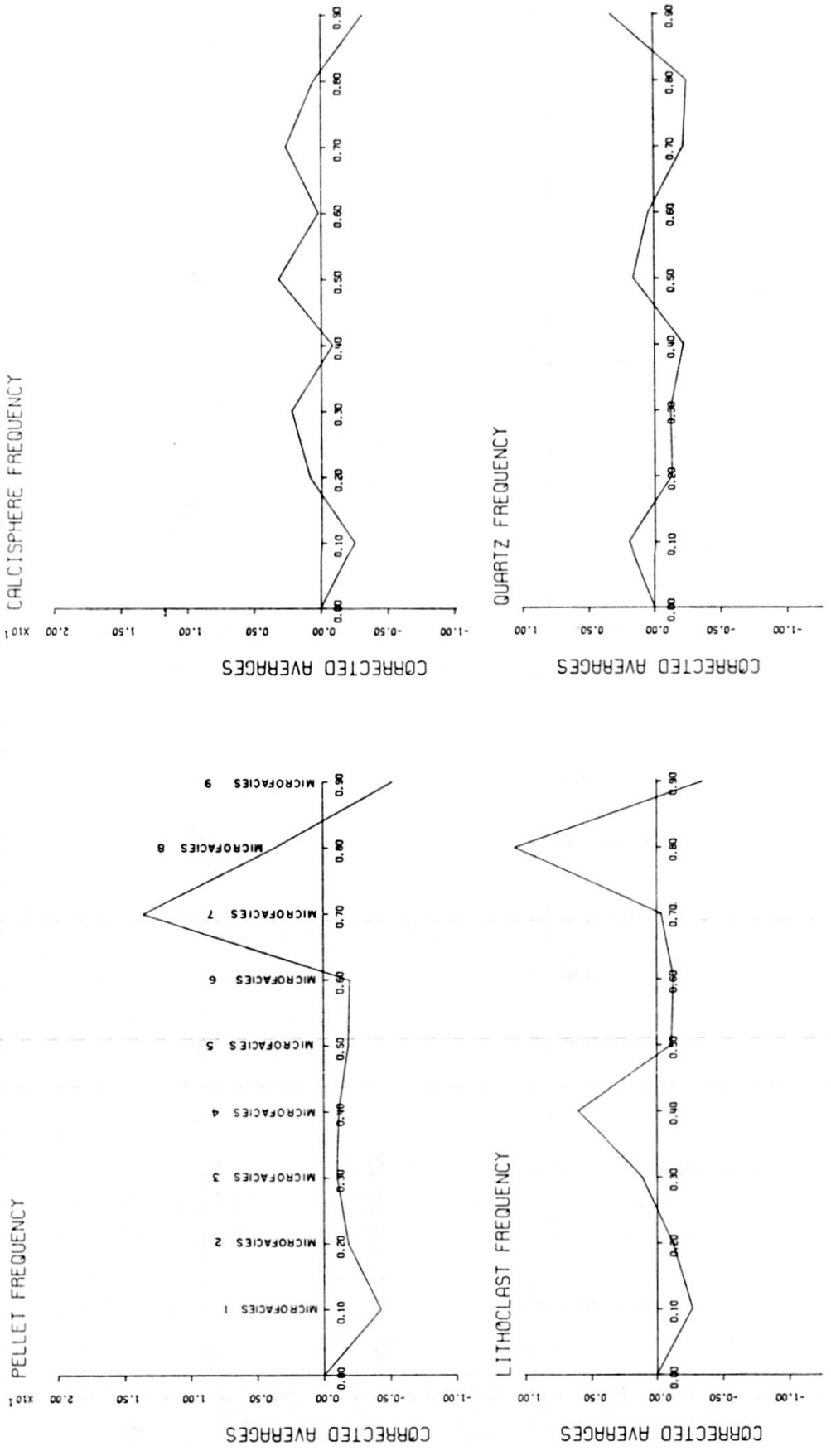

FIG. 10. — Variation of Coded Average Values of Parameters Through all Microfacies

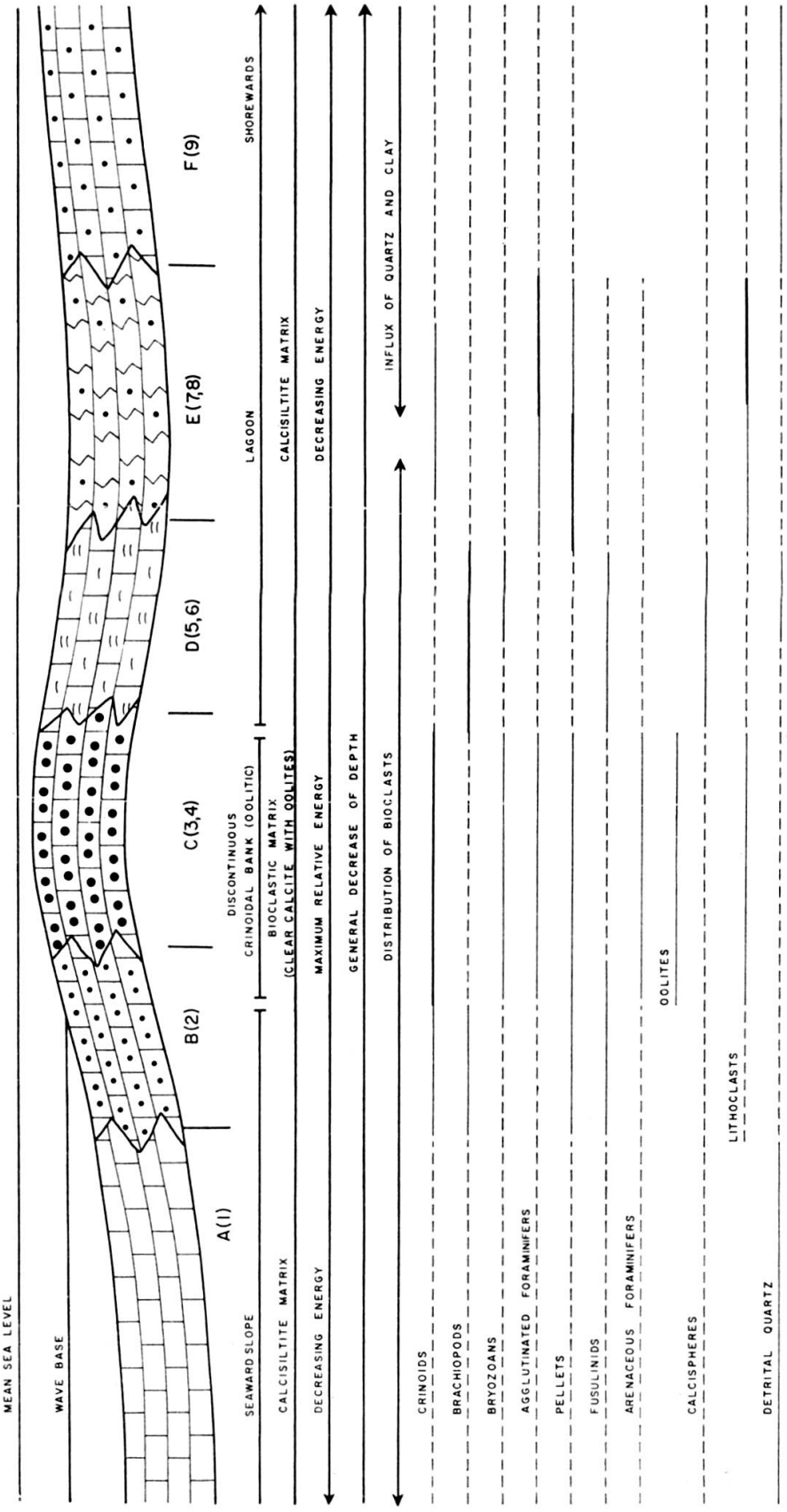

FIG. 11. — Horizontal Environmental Interpretation of Microfacies

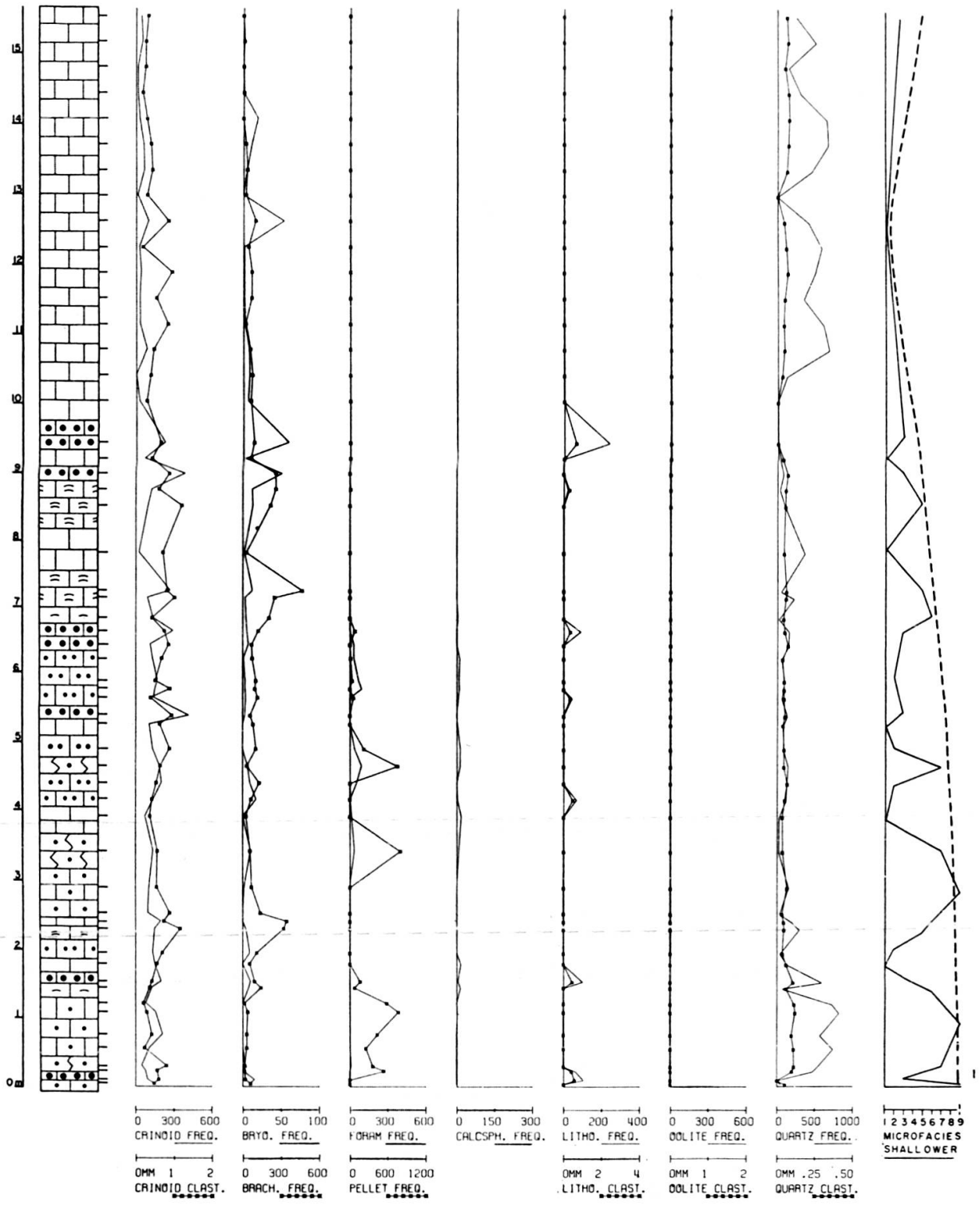

FIG. 12. — Parameter Curves for the Measured Section

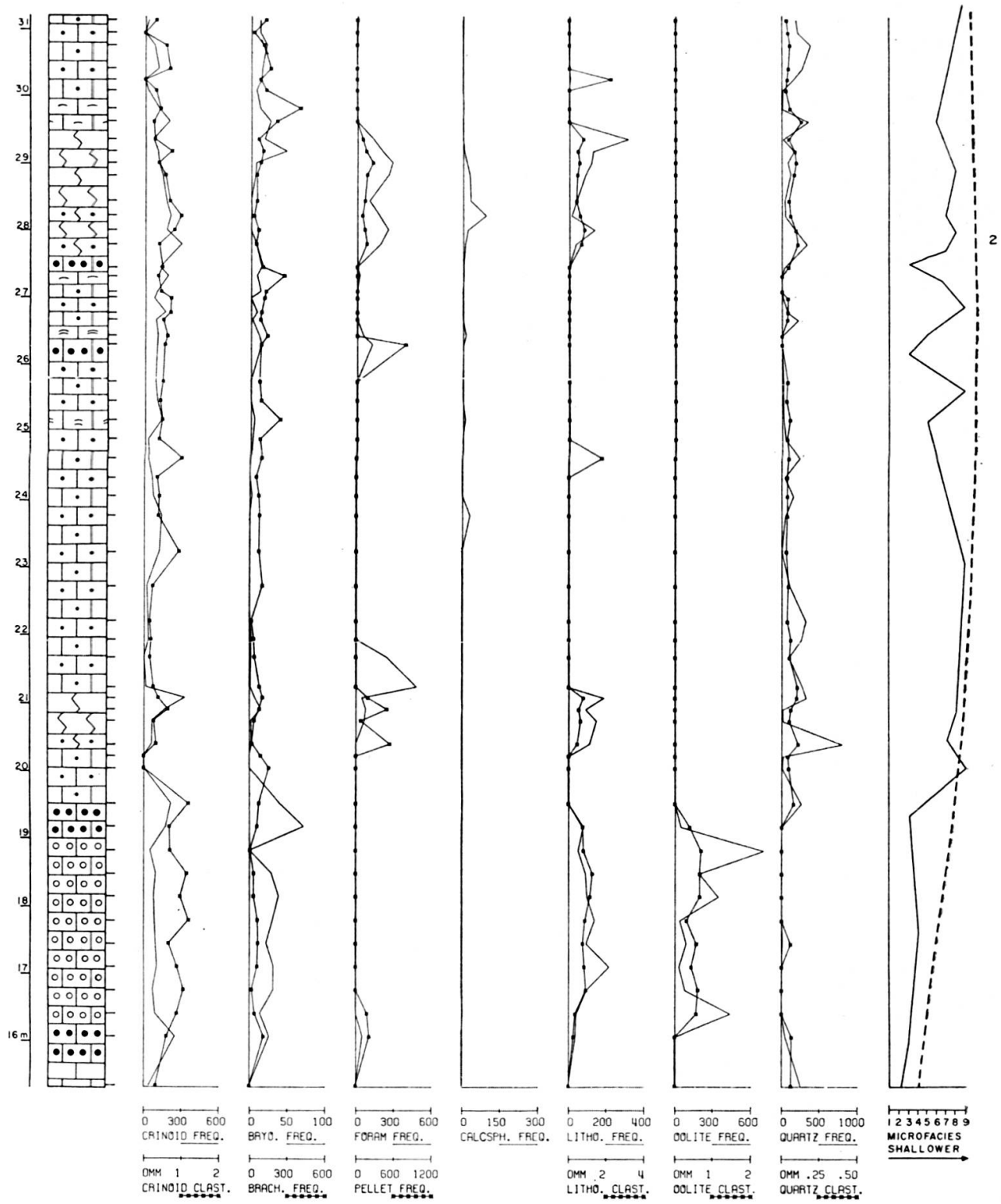

FIG. 13. — Parameter Curves for the Measured Section (Continued)

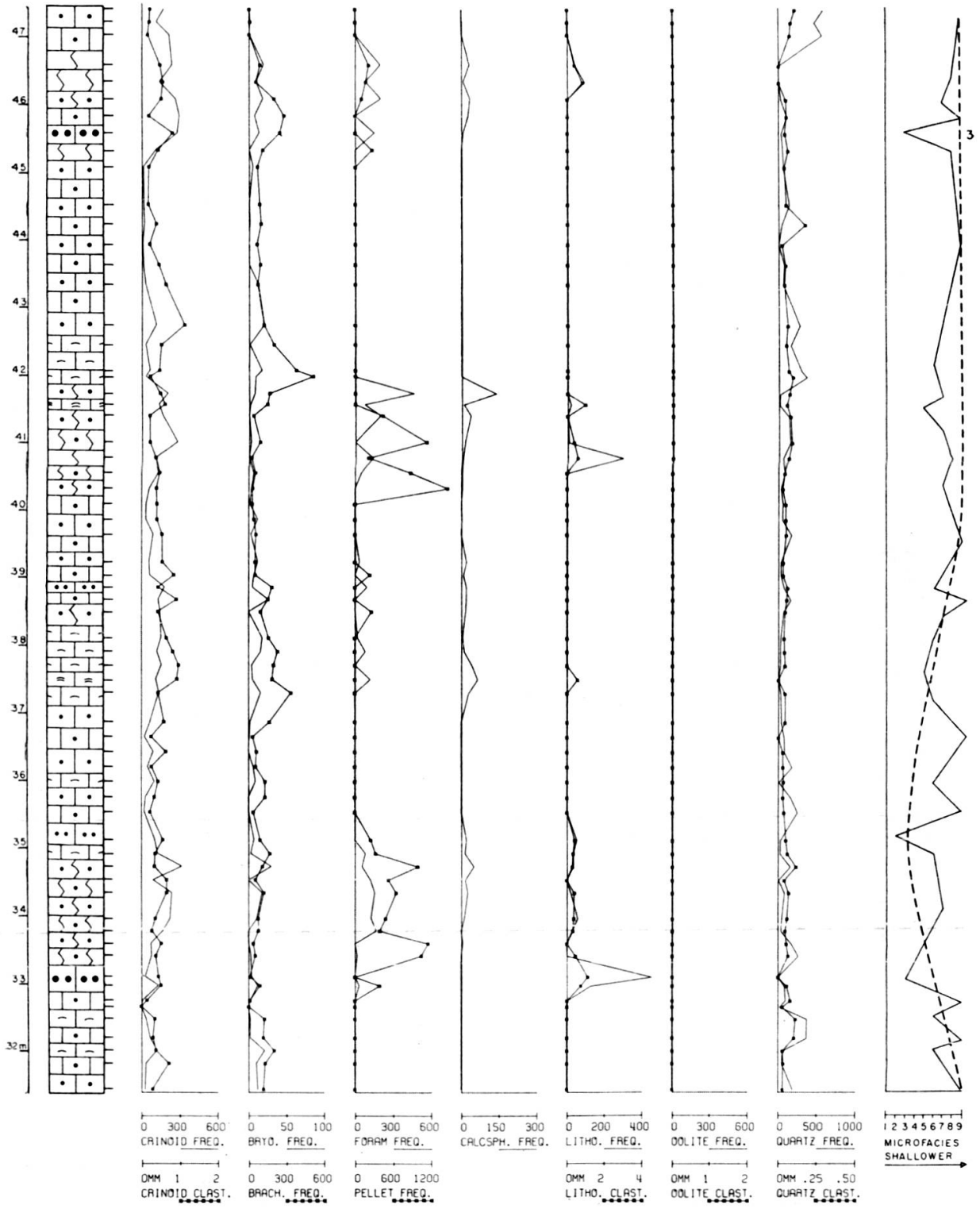

FIG. 14. — Parameter Curves for the Measured Section (Continued)

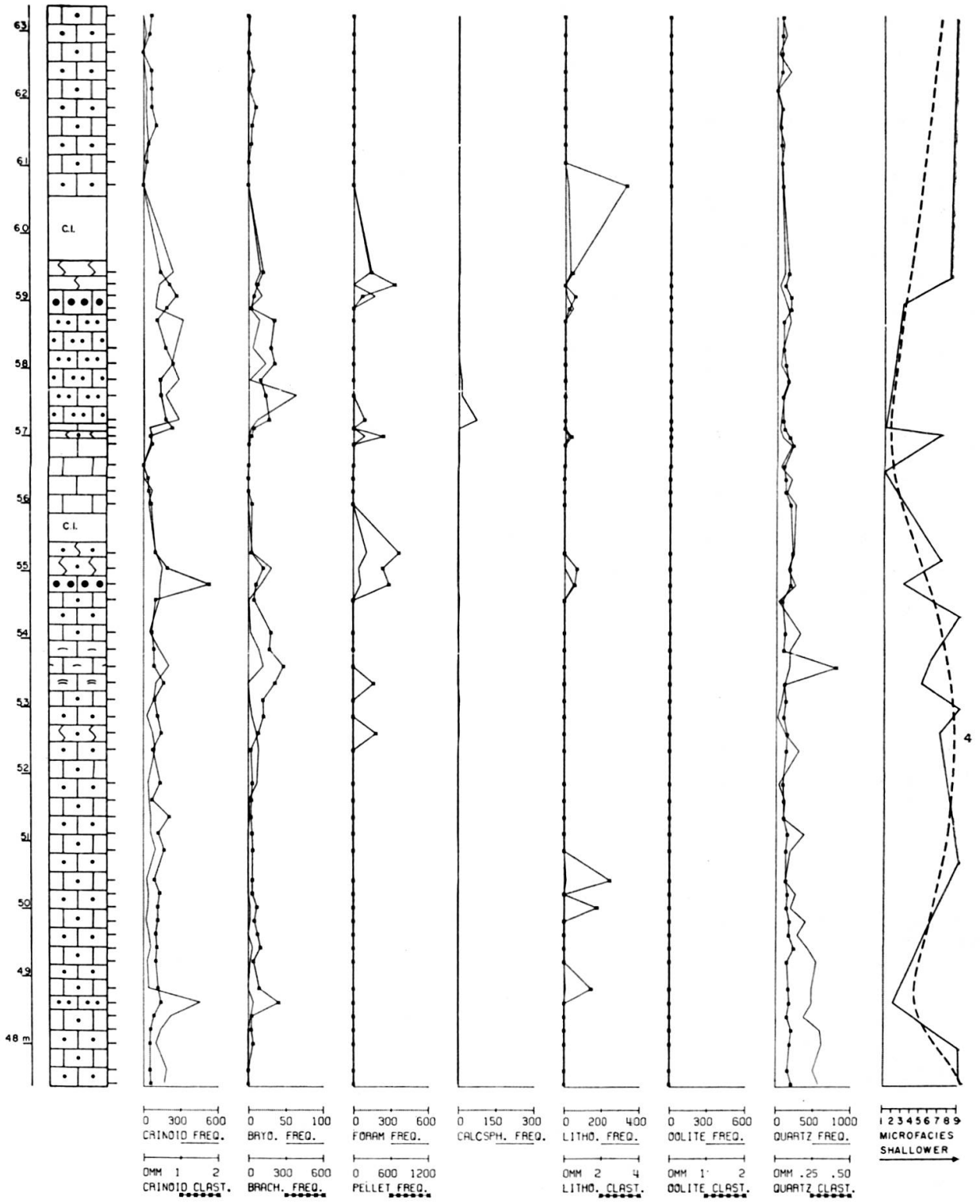

FIG. 15. — Parameter Curves for the Measured Section (Continued)

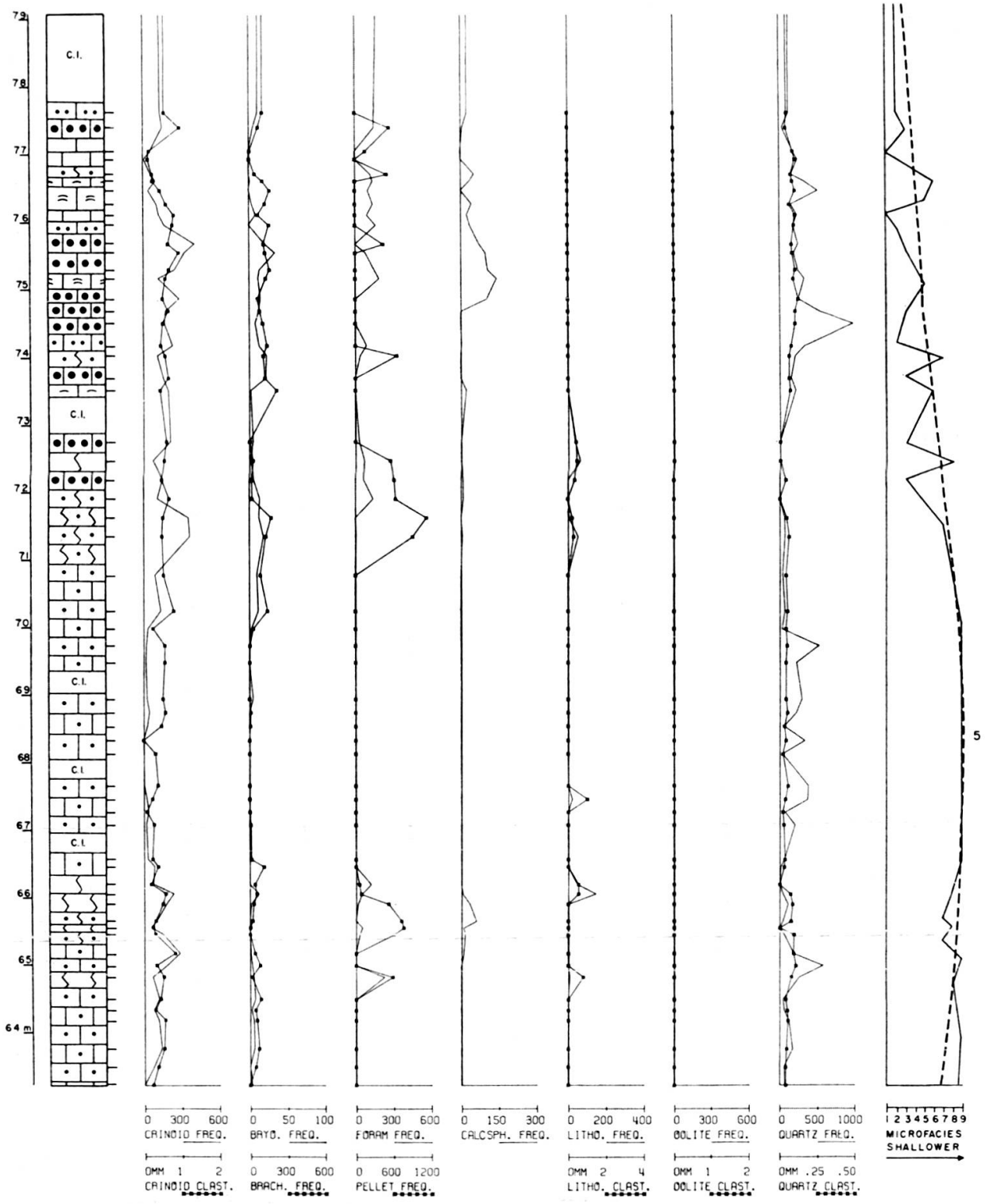

FIG. 16. — Parameter Curves for the Measured Section (Continued)

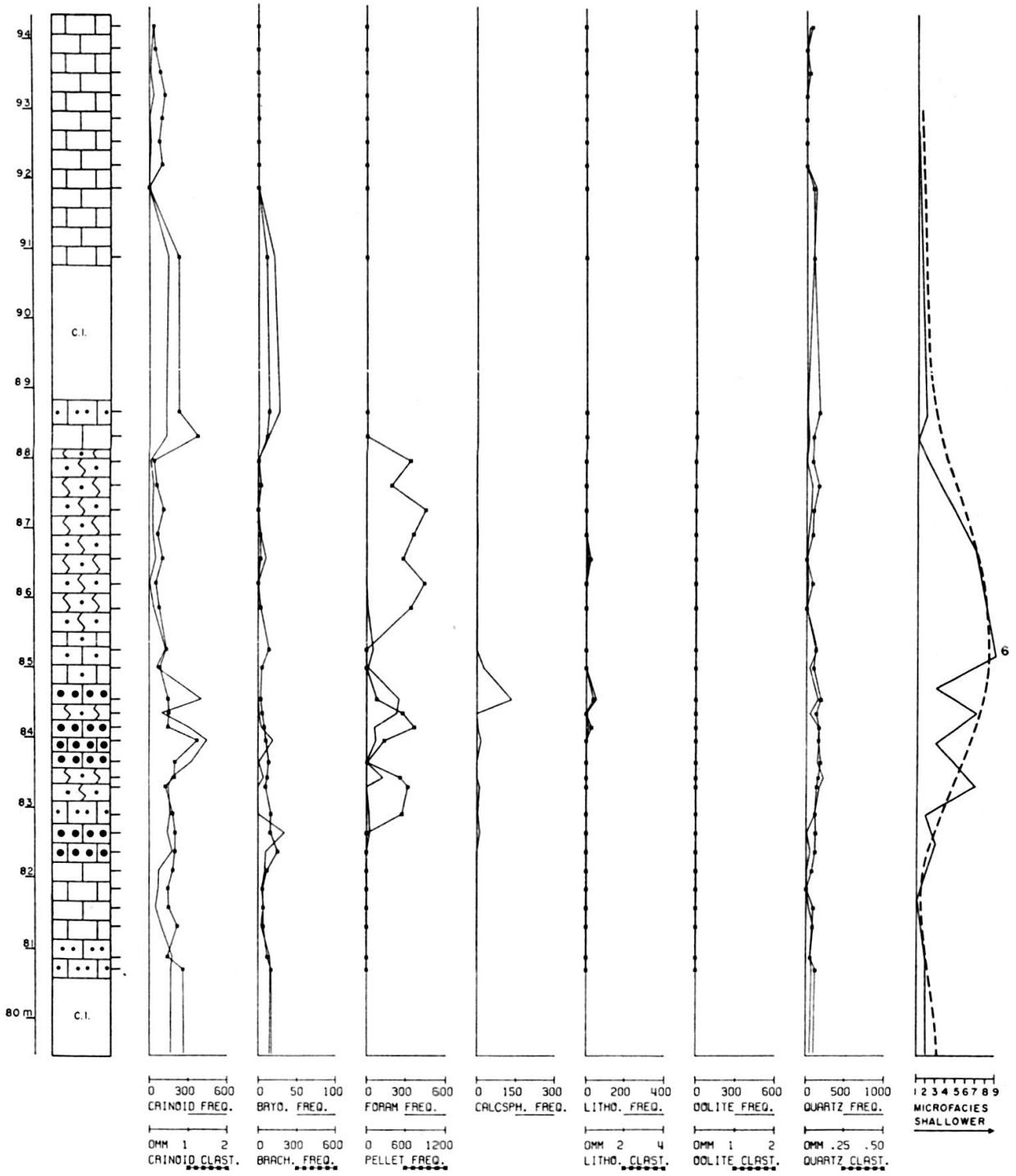

FIG. 17. — Parameter Curves for the Measured Section (Continued)

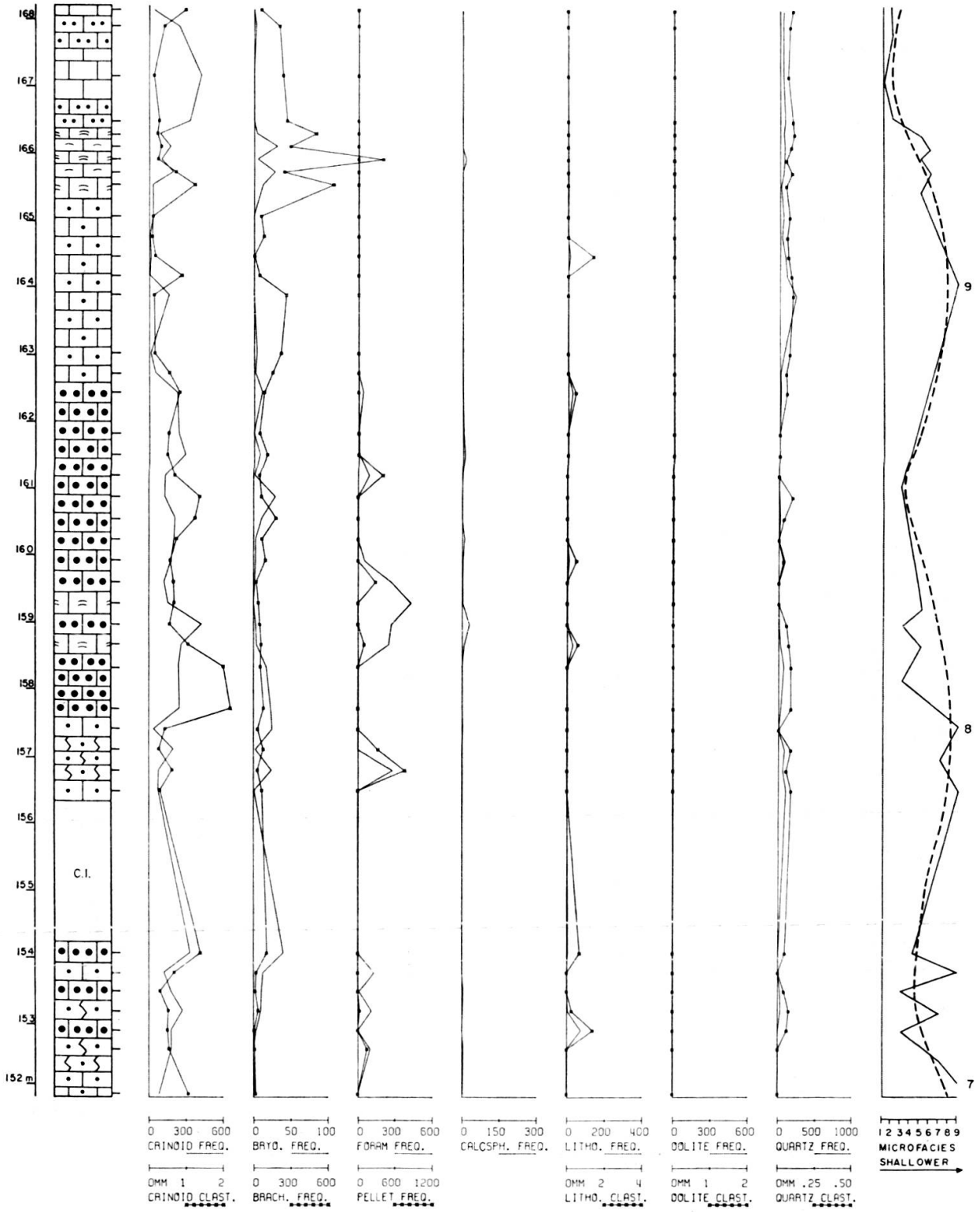

FIG. 18. — Parameter Curves for the Measured Section (Continued)

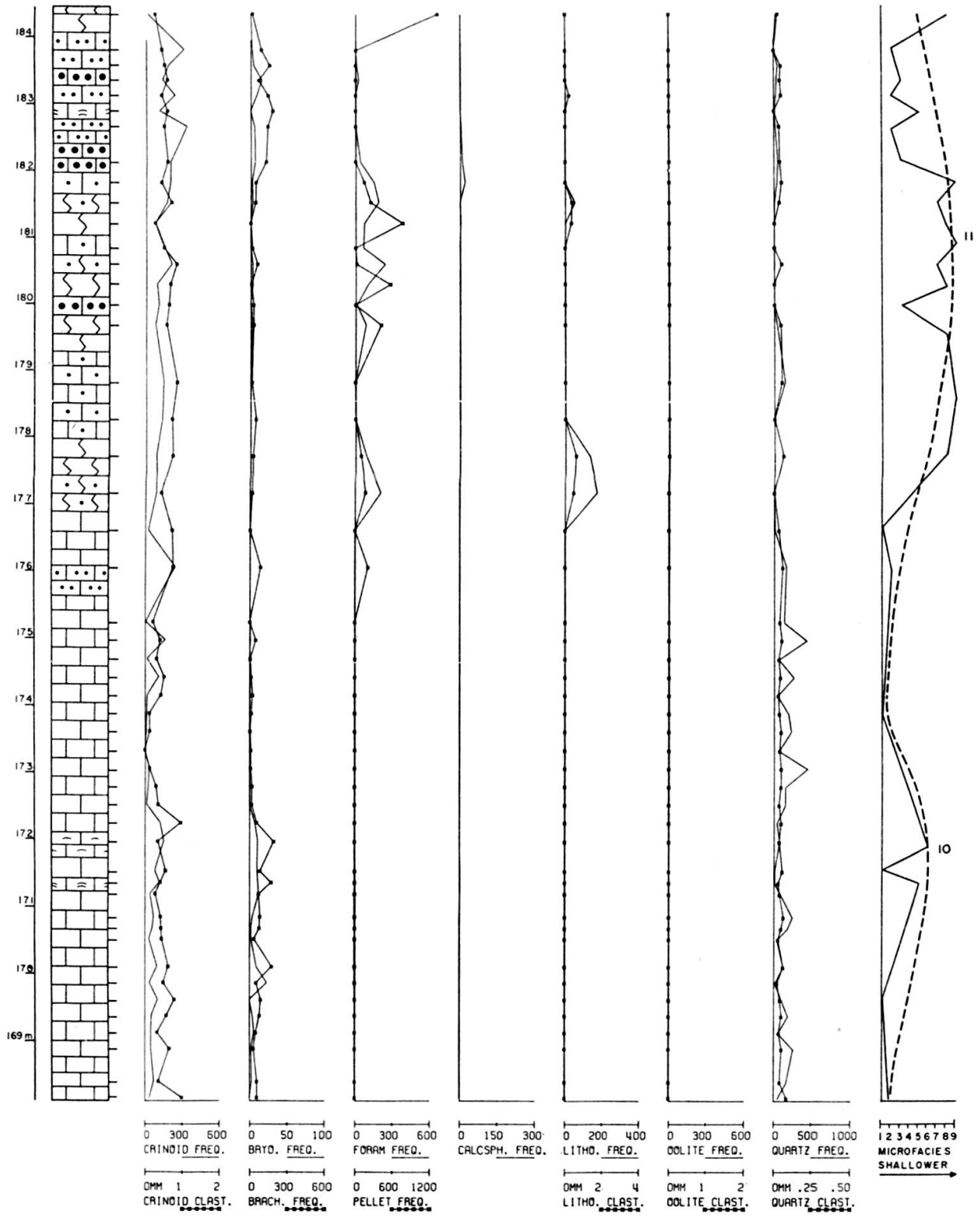

FIG. 19. — Parameter Curves for the Measured Section (Continued)

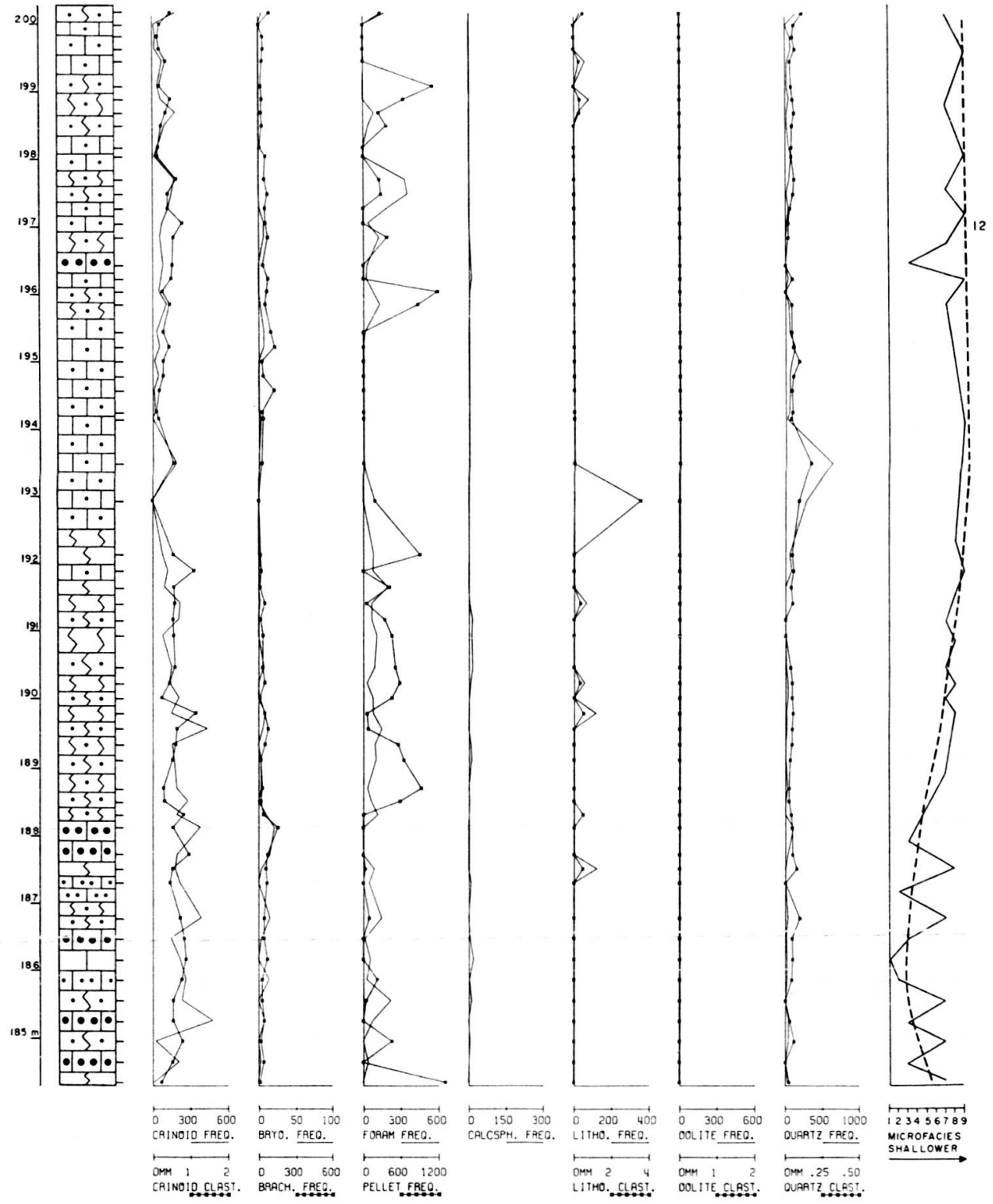

FIG. 20. — Parameter Curves for the Measured Section (Continued)

The curve of quartz frequency (Figure 10) shows three peaks, in microfacies 1, 6 and 9.

Coded average frequencies of components and relationships of the ideal vertical sequence can be used to make a final horizontal reconstruction (Figure 11) of the investigated stratigraphic section, showing the inferred relationship between wave base and type of interstitial material and the approximate concentrations of certain components.

Six sub-environments may be recognized:

Sub-environment A : A low energy area below wave base, represented by microfacies 1, a calcisiltite with few sand-size bioclasts but with a concentration of fine-grained detrital quartz.

Sub-environment B : An area of moderately high environmental energy extending from below wave base to slightly above it, represented by microfacies 2 which is a mud-supported biocalcarenite with either a micritic or a bioclastic matrix. Crinoids, brachiopods, and occasionally fusulinids are the most commonly found constituents.

Sub-environment C : It is formed by a discontinuous crinoidal bank or bar, at times oolitic, and displays the highest relative energy of the inferred environmental model. It is the source of much of the biogenic debris found in most other sub-environments. Microfacies 3 and 4, respectively a grain-supported biocalcarenite with a bioclastic matrix and an oolitic calcarenite with a cavity-filling sparry calcite cement, are representative of this sub-environment. This area is characterized by an abundance of crinoids, bryozoans, red algae, and lithoclasts. At times, agglutinated and arenaceous foraminifers and pellets are important constituents.

Sub-environment D : It corresponds to the back slope of the crinoidal bar and is characterized by relatively quiet water conditions. Microfacies 5, a grain-supported biocalcarenite with a calcisiltite matrix, and microfacies 6, mud-supported biocalcarenite with a calcisiltite matrix, are found here. Brachiopods are the most abundant organisms although fusulinids are common. This area acted as a trap for coarser grains of detrital quartz which were too large to be transported over the crinoidal bar.

Sub-environment E : This is the lagoon behind the crinoidal bar where microfacies 7, a fine-grained, pelletoidal calcarenite with a calcisiltite matrix, and microfacies 8, a pelletoidal and foraminiferal calcarenite with a calcisiltite matrix which is usually recrystallized to pseudospar, were deposited. Fecal pellets, agglutinated foraminifers, and lithoclasts are the most abundant constituents. This area is normally characterized by quiet water conditions although near-shore intraformational reworking can occur, forming small lithoclasts of pelletoidal micrite.

Sub-environment F: This is a shoreward portion of the lagoon and is represented by microfacies 9, a calcisiltite with few sand-size bioclasts. Samples from this area commonly display quartz-rich laminae and contain flat micrite desiccation chips.

DESCRIPTION OF THE MEASURED SECTION

The nine identified microfacies represent different environmental conditions that existed during the time of sediment deposition. The variation of microfacies within the measured section is shown by the inferred bathymetric curves on the left of Figures 12-20. The main trend of the oscillations between different microfacies is shown by a dashed line superposed on the bathymetric curve. Twelve large cycles, from deep water to shallow water and back to deep water conditions, were found. High points on the curve, corresponding to shallow water conditions, have been numbered from 1 to 12 starting at the base of the section.

The description of the cycles will be limited to noting features of particular interest or those that differ appreciably from the proposed ideal sequence. At the end of each description are 3 numbers; the first is the number of the microfacies at the base of that cycle; the second, the microfacies at the shallowest point reached in the cycle in question; and the third number is the microfacies at the top of the cycle.

Cycle one is an incomplete cycle wich extends below the investigated section and is a continuation of an incomplete cycle at the top of the previously described lower portion of the Bird Spring Group. In the deepening phase are numerous oscillations with decreasing amplitude ((-9-1).

Cycle two (23 meters thick) is a symmetric cycle which shows two aspects. In the shallowing phase, the gradual decrease of water depth is followed by an abrupt shallowing. The deepening phase is very complex and has numerous small amplitude oscillations (1-9-2).

Cycle three (13 meters thick) is symmetric with abrupt deepening and shallowing phases and many oscillations at its peak (2-9-2).

Cycle four (9 meters thick) is a short asymmetric cycle with a short shallowing phase and a deepening phase marked by several small oscillations (2-9-1).

Cycle five (24 meters thick) is a long asymmetric cycle. There are numerous oscillations with decreasing amplitude in the deepening phase, similar in character to those found in cycle one (1-9-1).

Cycle six (12 meters thick) is a short, relatively simple, symmetric cycle (1-9-1-).

Between cycles six and seven, extends a completely dolomitized sequence, 58 meters thick, in which it was not possible to assign samples to microfacies.

Cycle seven is an incomplete cycle which started in the dolomite sequence (-9-3).

Cycle eight (8 meters thick) is a short, symmetric cycle with small amplitude oscillations in the deepening phase (3-9-3).

Cycle nine (8 meters thick) is a short, symmetric cycle (3-9-1).

Cycle ten (7 meters thick) has the smallest amplitude of all described cycles. It is asymmetric, with a long shallowing phase and a short deepening phase (1-6-1).

Cycle eleven (11 meters thick) is asymmetric with an abrupt shallowing phase and a deepening phase marked by many high amplitude oscillations (1-9-1).

Cycle twelve is an incomplete cycle extending above the investigated section. The shallowing phase is marked by several small oscillations with increasing amplitude (1-9-).

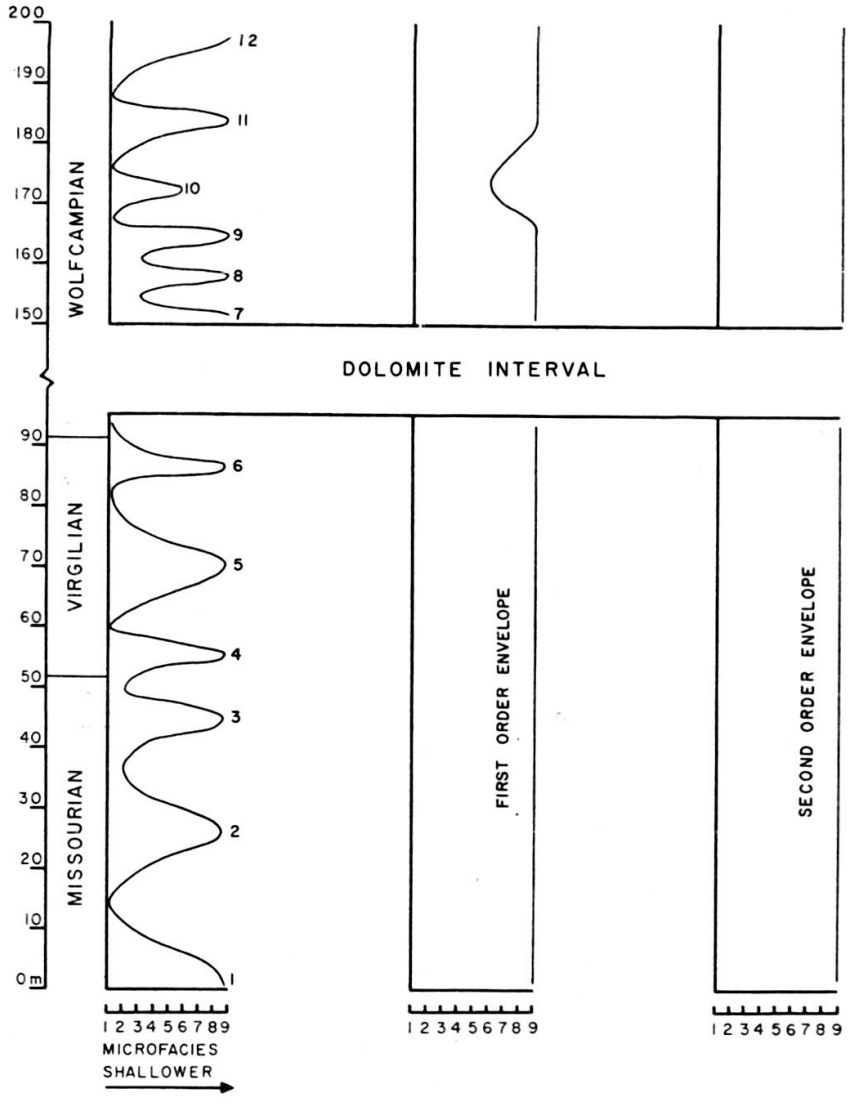

FIG. 21. — Generalized Relative Bathymetric Curves for Investigated Section

COMPARISON WITH PREVIOUS INVESTIGATIONS

The present investigation has shown that the upper portion of the Bird Spring Group consists of 12 cycles (Figure 21) which correspond to oscillations of water depth. This pattern of cyclic sedimentation is a continuation of the cyclicity found in the lower part of the Bird Spring Group (HEATH, LUMSDEN, and CAROZZI, 1967), however there are differences in the nature of the cycles. In the present study, the average thickness of cycles is 13 meters whereas in the lower part of the Bird Spring Group the average cycle thickness is only 8 meters.

The first order envelope (Figure 21), drawn as a tangent to the maxima of the preceding curve, is essentially a straight line and the second order envelope curve (Figure 21), drawn as a tangent to the first order envelope curve, is a straight line. Both envelope curves indicate that the investigated sequence had no overall deepening

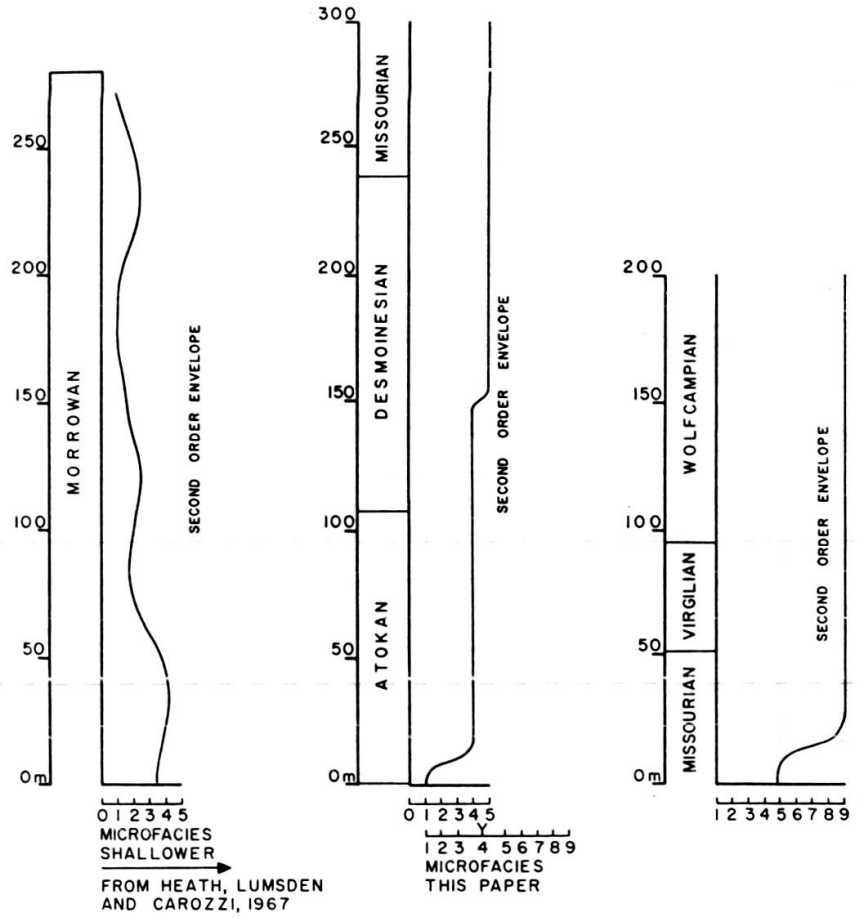

FIG. 22. — Generalized Relative Bathymetric Curves for Morrowan through Wolfcampian

or shallowing trends and that the upper portion of the Bird Spring Group was deposited in a stable, shallow environment. In contrast, the 562 meters of the Bird Spring Group directly below the investigated section is a major transgressive-regressive sequence, with transgression occurring during Morrowan and regression during Atokan through Lower Missourian.

Comparing the generalized relative bathymetric curves for the Morrowan through Wolfcampian with each other (Figure 22) brings out two points. The entire sequence represents a major transgression and regression with the investigated section in the upper part of the regression. During the Morrowan the general transgression is marked by several small amplitude oscillations. The interval Atokan through Lower Missourian shows the regression occurring in two steps and without the oscillations of the previous section. During Upper Missourian through Wolfcampian the general relative bathymetry does not change.

CONCLUSIONS

The upper portion of the Bird Spring Group (Upper Missourian-Wolfcampian) consists of 9 distinct carbonate microfacies which grade into each other vertically and horizontally. Considered together they can be used to construct an environmental model for the deposition of the stratigraphic interval in question. The model, which can be subdivided into 6 sub-environments, consists of a seaward slope which grades into a discontinuous crinoidal bar and a lagoon located behind the bar.

Cyclic sedimentation, which was found in the lower portion of the Bird Spring Group, continues in the investigated section. The 9 microfacies are repeated in 12 major cycles corresponding to oscillations of water depth. The regression, which was found in the interval Atokan through Lower Missourian, continues through the interval Upper Missourian through Wolfcampian. However the 12 cycles recognized within the latter interval have similar amplitudes, indicating no tendency for further shallowing.

APPENDIX

To test the validity of a vertical sampling interval of 20 cm for adequately distinguishing microfacies, a 15 meter vertical section was sampled as closely as possible (176 samples) to approximate a continuously sampled section. In the laboratory this continuously sampled section was resampled at approximately a 20 cm interval (68 samples) to simulate sampling of the rest of the section.

With a 20 cm sampling interval, 33 microfacies were recognized in the 15 meter section; the average thickness of these 33 microfacies was 47 cm. In contrast, when all 176 samples were considered, 75 microfacies, with an average thickness of 21 cm, were recognized.

To determine the statistical significance of the difference between the average thickness of recognized microfacies of the two groups, a *t*-test was used. The null hypothesis, *Ho*, is that the average thickness of microfacies with a 20 cm sampling

interval is the same as the average microfacies thickness using continuous sampling; or $Ho: \mu_1 = \mu_2$. The alternative hypothesis, *Ha*, is that the average thickness of microfacies using a 20 cm sampling interval is greater than the average microfacies thickness using continuous sampling; or $Ha: \mu_1 > \mu_2$. The unbiased estimators of population means μ_1 and μ_2 are the two sample means mentioned above.

The test statistic used is:

$$t = \frac{\overline{Y}_1 - \overline{Y}_2}{S_d}$$

where $\overline{Y}_1$ is the average microfacies thickness using a 20 cm sampling interval, $\overline{Y}_2$ is the average microfacies thickness using continuous sampling, and S_d is the standard deviation of the difference between the two means.

A summary table for the *t*-test is given below.

Sample	N	df	$\overline{Y}$	Sum of squares
1	68	67	46.95	212663
2	176	175	20.93	550823
		242		763486

where N is the number of thin sections in each sample, df is degrees of freedom, $\overline{Y}$ is the average (in centimeters) microfacies thickness. The sum of squares was calculated using the following formula:

$$\text{sum of squares} = m_i (Y_i - \overline{Y})^2$$

where m_i is the number of thin sections in the i^{th} microfacies, Y_i is the thickness of that microfacies, and $\overline{Y}$, is the average microfacies thickness.

Assuming that variance for both sample populations is the same, the best estimator of population variance is the pooled variance, S^2.

$$S^2 = \frac{\text{pooled sum of squares}}{\text{pooled } df} = \frac{m_j (Y_{1j} - \overline{Y}_1)^2 + m_k (Y_{2k} - \overline{Y}_2)^2}{N_1 + N_2 - 2}$$

The estimated variance of the difference between the two means is $S_d^2 = S^2 (1/N_1 + 1/N_2)$. For the two samples in question,

$$S^2 = \frac{763486}{242} = 3154$$

$$S_d^2 = 3154 (1/68 + 1/176) = 64.3$$

$$S_d = 8.01$$

The calculated t value in this case is:

$$t = \frac{\overline{Y}_1 - \overline{Y}_2}{S_d} = \frac{46.95 - 20.93}{8.01} = 3.24$$

To test the hypothesis that a significant difference exists between sample means, t calculated is compared to tabulated t values. If t calculated exceeds t tabulated, the difference between average microfacies thickness cannot be attributed to random error and it must be concluded that a significant difference between the two exists. The value of t tabulated at the .5% level of significance is 2.576, smaller than t calculated. The null hypothesis is rejected, therefore the difference is concluded to be statistically significant.

LIST OF REFERENCES

BISSELL, J. J. (1962). Pennsylvanian and Permian rocks of the Cordilleran area, in *Pennsylvanian System in the United States*, C. C. Branson, Ed.: Am. Assoc. Petroleum Geologists, Tulsa, Oklahoma, pp. 188-263.

BRILL, K. G. (1963). Permo-Pennsylvanian stratigraphy of western Colorado Plateau and Eastern Great Basin regions: *Geol. Soc. America Bull.*, v. 74, pp. 307-333.

CAROZZI, A. V. (1950). Contributions à l'étude des rythmes de sédimentation: *Archives des Sciences*, Genève. v. 3, pp. 1-76.

—— (1958). Micro-mechanisms of sedimentation in the epicontinental environment: *Jour. Sed. Petrology*, v. 28, pp. 133-150.

—— (1960). *Microscopic Sedimentary Petrography:* John Wiley and Sons, Inc., New York, 485 p.

—— (1961). Reef petrography in the Beaverhill Lake Formation, Upper Devonian, Swan Hills area, Alberta, Canada: *Jour. Sed. Petrology*, v. 31, pp. 497-513.

CASSITY, P. E. (1965). Pennsylvanian and Permian fusulinids of the Bird Spring Group from Arrow Canyon, Clark County, Nevada: *Unpubl. MS thesis, University of Illinois*, 112 p.

—— and R. L. LANGENHEIM, Jr. (1966). Pennsylvanian and Permian fusulinids of the Bird Spring Group, Clark County, Nevada: *Jour. Paleontology*, v. 40, pp. 931-968.

DOTT, R. H., Jr. (1958). Cyclic pattern in mechanically deposited Pennsylvanian limestones of northeastern Nevada: *Jour. Sed. Petrology*, v. 28, pp. 3-14.

FOLK, R. L. (1962). Spectral subdivision of limestone types, in *Classification of Carbonate Rocks*, W. E. Ham, Ed.: Am. Assoc. Petroleum Geologists, Memoir No. 1, Tulsa, Oklahoma, pp. 62-84.

HEATH, C. P. M., D. N. LUMSDEN and A. V. CAROZZI (1967). Petrography of a carbonate transgressive-regressive sequence: the Bird Spring Group (Pennsylvanian), Arrow Canyon Range, Clark County, Nevada: *Jour. Sed. Petrology*, v. 37, pp. 377-400.

KAY, M. (1947). Geosynclinal nomenclature and the craton: *Am. Assoc. Petroleum Geologists Bull.*, v. 31, pp. 1289-1293.

LANGENHEIM, R. L., Jr., B. W. CARSS, J. B. KENNERLY, V. A. MCCUTCHEON and R. H. WAINES (1962). Paleozoic section in Arrow Canyon Range, Clark County, Nevada: *Am. Assoc. Petroleum Geologists Bull.*, v. 46, pp. 592-609.

LANGENHEIM, V. A. M. and R. L. LANGENHEIM Jr. (1965). The Bird Spring Group, Chesterian through Wolfcampian at Arrow Canyon, Arrow Canyon Range, Clark County, Nevada: *Trans. Ill. State Acad. Sci.*, v. 58, No. 4., pp. 225-240.

MAMET, B. L. (1970). Carbonate microfacies of the Windsor Group (Carboniferous), Nova Scotia and New Brunswick: *Geol. Surv. Can., Paper 70-21*, 120 p.

RAO, C. P. (1970). Application of computer techniques to the petrographic study of oolitic environments, Ste Genevieve Limestone (Mississippian), southern Illinois and eastern Missouri: *Unpubl. Ph. D. thesis, University of Illinois*, 105 p.

—— and A. V. CAROZZI (1971). Application of computer techniques to the petrographic study of oolitic environments, Ste Genevieve Limestone (Mississipian), southern Illinois and eastern Missouri: *Archives des Sciences*, Genève, v. 24, No. 1. pp. 17-55.

RICH, M. (1969). Petrographic analysis of Atokan carbonate rocks in central and southern Great Basin: *Am. Assoc. Petroleum Geologists Bull.*, v. 53, pp. 340-366.

—— (1971). Middle Pennsylvanian rocks of eastern Great Basin: *Am. Assoc. Petroleum Geologists Bull.*, v. 55, pp. 432-453.

WEBSTER, G. D. (1969). Chester through Derry conodonts and stratigraphy of northern Clark and southern Lincoln Counties, Nevada: *Univ. Calif. Publ. Geol. Science*, No. 79, 121 p.

WELSH, J. E. (1959). Biostratigraphy of the Pennsylvanian and Permian Systems in southern Nevada: *Unpubl. Ph. D. thesis, University of Utah*, 106 p.

WRAY, J. L. (1965). Calcareous algae in limestones of the Lansing Group, in *Pennsylvanian marine banks in southeastern Kansas*: Field Conference Guidebook, Geol. Soc. America, pp. 47-54.

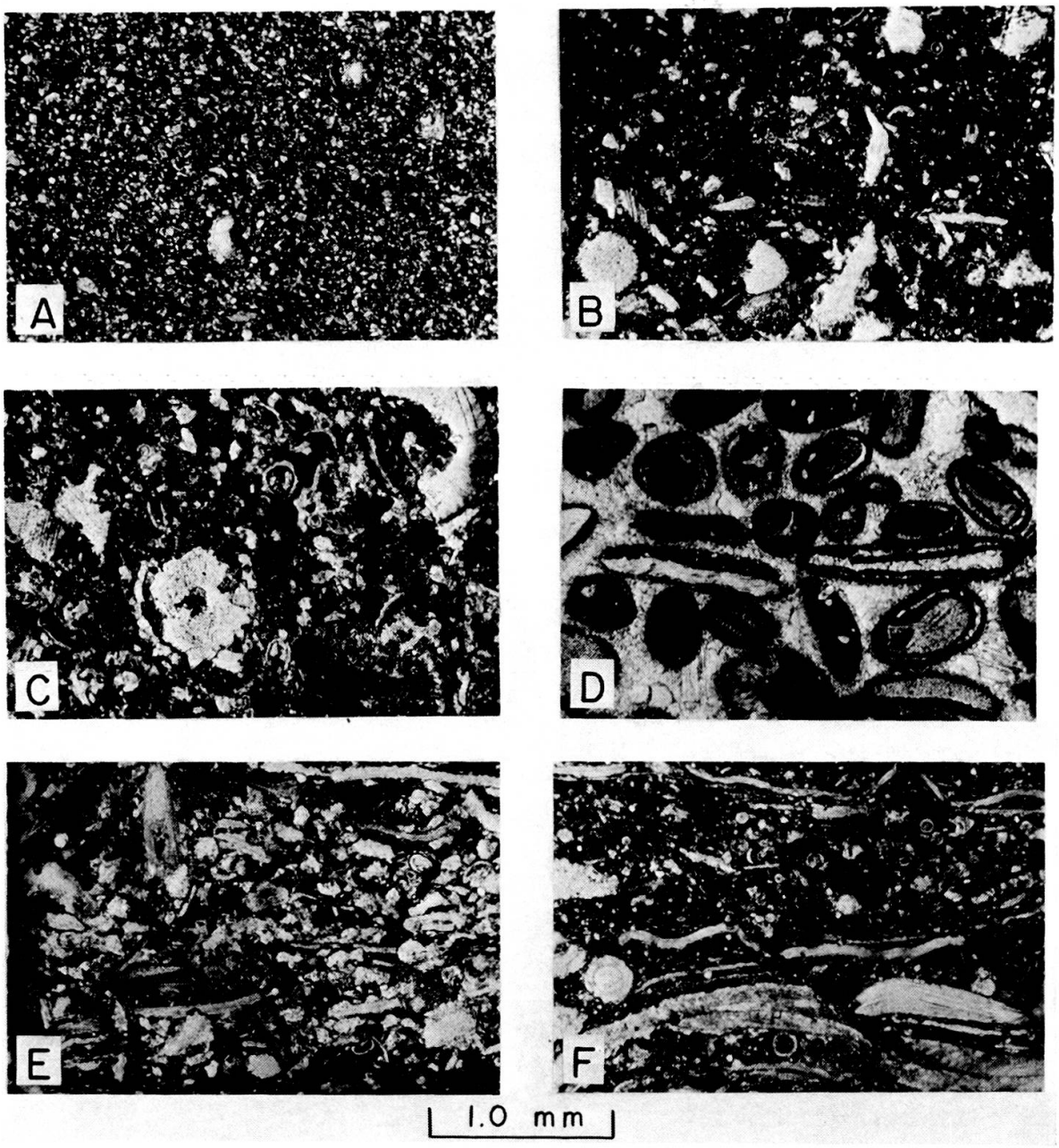

A. Calcisiltite with scattered sand-size bioclasts (Microfacies 1).
B. Mud-supported crinoidal calcarenite with calcisiltite matrix (Microfacies 2).
C. Grain-supported crinoidal calcarenite with pelletoidal bioclastic matrix (Microfacies 3).
D. Oolitic calcarenite with cavity-filling sparry calcite cement (Microfacies 4).
E. Grain-supported brachiopod calcarenite with calcisiltite matrix (Microfacies 5).
F. Mud-supported brachiopod calcarenite with calcisiltite matrix (Microfacies 6).

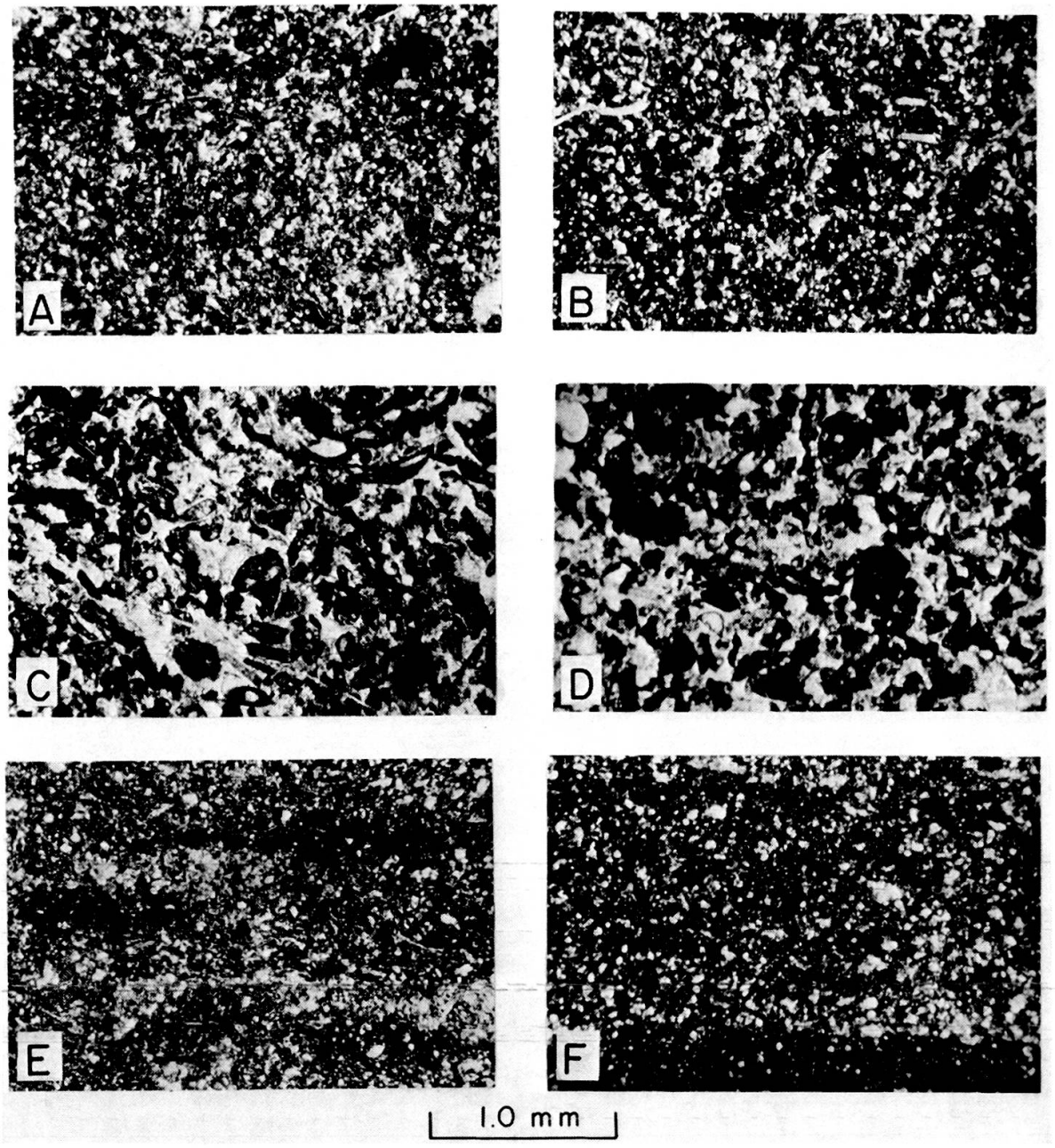

A and B. Fine grained pelletoidal calcarenite with calcisiltite matrix, showing bioturbation and merging of pellets (Microfacies 7).

C and D. Pelletoidal and foraminiferal calcarenite with calcisiltite matrix recrystallized to pseudospar, abundant agglutinated foraminifers and lithoclasts of pelletoidal micrite (Microfacies 8).

E. Calcisiltite with flat, micritic desiccation chips (Microfacies 9).

F. Laminated calcisiltite showing quartz-rich layer (Microfacies 9).